SOME CRYSTAL STRUCTURES
OF
CYCLOPENTADIENYL PERFLUOROALKYL TRIPHENYLPHOSPHINE
METAL COMPLEXES

SALINA SIK-CHOW CHEUNG

A THESIS
IN
THE DEPARTMENT
OF
CHEMISTRY

Presented in Partial Fulfillment of the Requirement
for the Degree of Master of Science at
Concordia University
Sir George Williams Campus
Montreal, Canada
April, 1975

ABSTRACT

SOME CRYSTAL STRUCTURES OF CYCLOPENTADIENYL PERFLUOROALKYL TRIPHENYL PHOSPHINE METAL COMPLEXES

SALINA SIK-CHOW CHEUNG

CONCORDIA UNIVERSITY

SIR GEORGE WILLIAMS CAMPUS, 1975.

This thesis describes three crystal structure determinations. The compounds studied are : π-$C_5H_5Fe(CO)(PPh_3)[CF(CF_3)_2]$, π-$C_5H_5Fe(CO)(PPh_3)(CF_2CF_3)$, and π-$C_5H_5Co(I)(PPh_3)(CF_2CF_3)$. The three compounds are structurally very similar, having the so-called "piano stool" configuration :

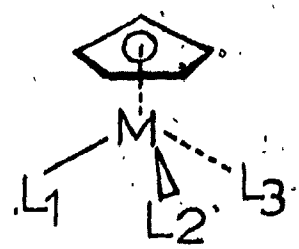

The results have been analyzed in terms of the rotational conformation with respect to the metal fluoroalkyl carbon σ - bond, and the chirality of the phosphorus center of asymmetry relative to that on the metal atom.

TABLE OF CONTENTS

LIST OF TABLES

LIST OF FIGURES

SECTION I GENERAL INTRODUCTION

The purpose of this thesis is to present the crystal structure of three compounds done by x-ray diffraction methods. The three compounds are :

(1) : π-$C_5H_5Fe(CO)(PPh_3)CF(CF_3)_2$ named Fluorfe 1

(2) : π-$C_5H_5Fe(CO)(PPh_3)CF_2CF_3$ named Fluorfe 2

(3) : π-$C_5H_5CoI(PPh_3)CF_2CF_3$ named Fluorco

The methods of preparing (1) and (2) are similar. They involve the replacement of a carbonyl group in π-$C_5H_5Fe(CO)_2C_3F_7$ and π-$C_5H_5Fe(CO)_2C_2F_5$ by a triphenylphosphine molecule respectively.(62,63)

$$\pi\text{-}C_5H_5Fe(CO)_2C_3F_7 \xrightarrow[h\nu\ 20^\circ C]{+\ P(C_6H_5)_3} \pi\text{-}C_5H_5Fe(CO)(PPh_3)C_3F_7$$

$$\pi\text{-}C_5H_5Fe(CO)_2(C_2F_5) \xrightarrow[h\nu\ 20^\circ C]{+\ P(C_6H_5)_3} \pi\text{-}C_5H_5Fe(CO)(PPh_3)C_2F_5$$

where π-$C_5H_5Fe(CO)_2C_3F_7$ and π-$C_5H_5Fe(CO)_2C_2F_5$ are both orange compounds synthesized from the decarbonylation of the fluoroacylmetal complex.(63)

The third compound, π-$C_5H_5CoI(PPh_3)C_2F_5$ was prepared(64)

from triphenylphosphine (0.30 g, 1.14 moles) and π-$C_5H_5Co(CO)(C_2F_5)I$ (0.3 g, 0.67 mole) in 50 ml of benzene. The reactants were heated in benzene for 2 hours at 50°. After the solvent was removed in vacuo the black crystalline product was purified by recrystallization from a benzene petroleum ether mixture, (0.25 g, 60% yield).

The compounds have the following common features ; they are all π-cyclopentadienyl derivatives, the metals are four co-ordinated and have triphenyphosphine as a ligand. Fluorfe 1 AND Fluorfe 2 both have a carbonyl group, while Fluorco is co-ordinated to Iodine.

There are two points of particular interest in these compounds, which are also under investigation by Dr. M.C. Baird of Queen's University :

(a) : The angles of rotation about Fe-C bond, which he is attempting to correlate with the N.M.R P-F coupling constants. See FIG.(1). It should be noted that it is a little dangerous to correlate solid state data (from a crystallographic structure) with solution data obtained from N.M.R.

(b) : The infrared spectra of some triphenylphosphine complexes of this type show two carbonyl frequencies where only one is expected (in solution). This is believed to originate from

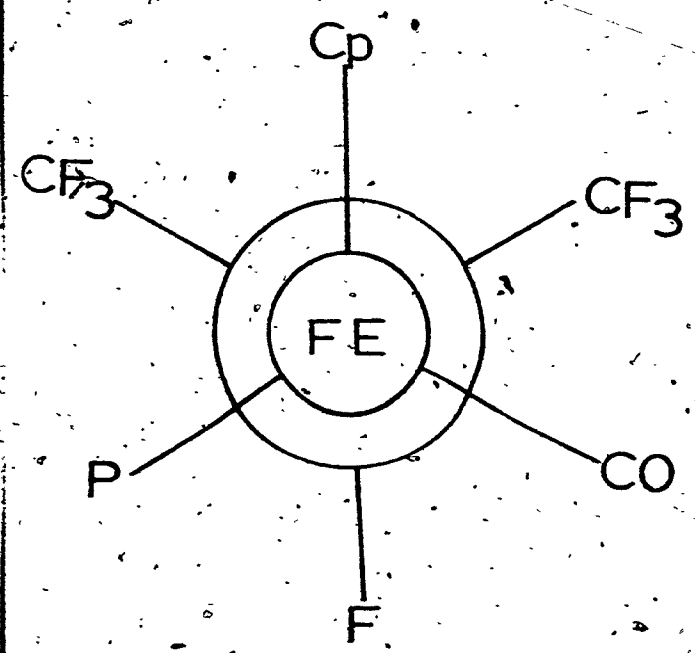

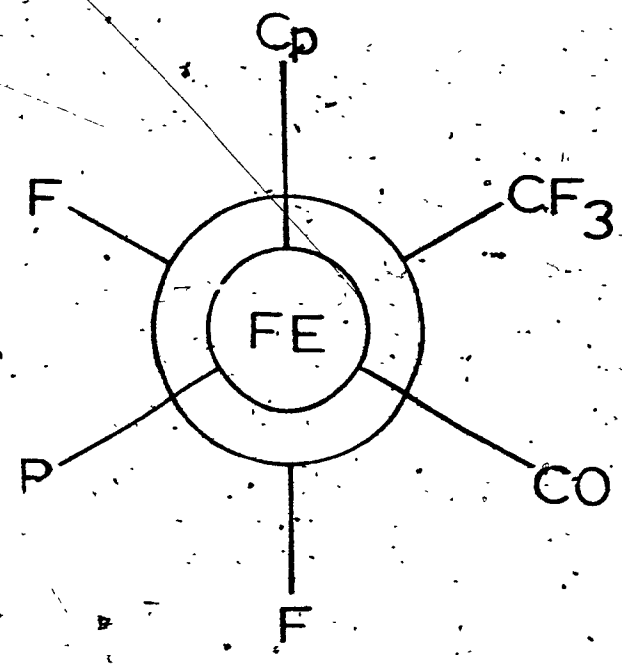

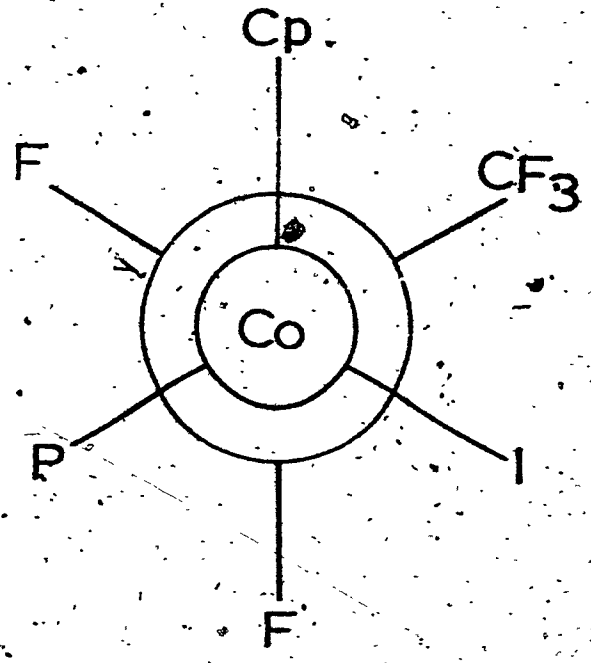

FIG(I)

the two possible chiralities of the $P(Ph_3)$ 'propeller' combined with the asymetric centre on Fe illustrated as the following figures :

(1)

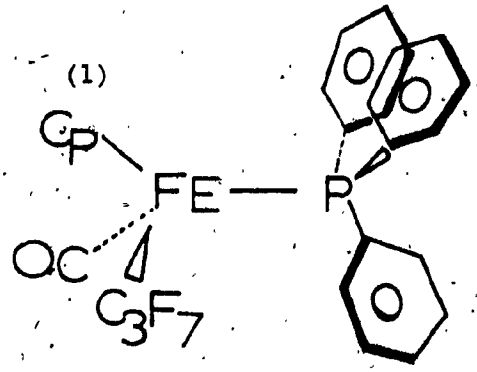

left hand screw

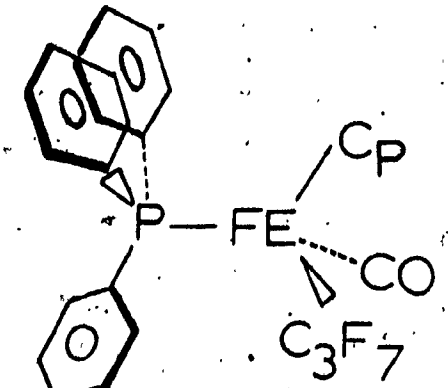

right hand screw

these two isomers have the same I.R.

(2)

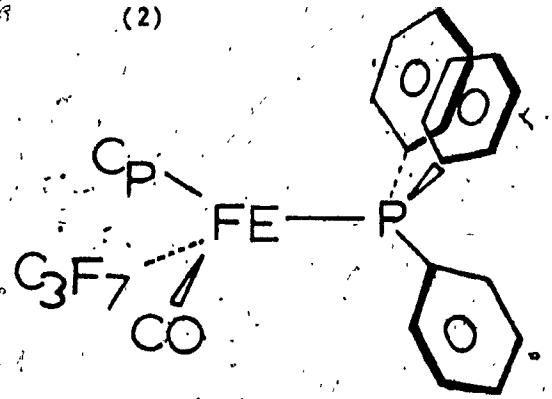

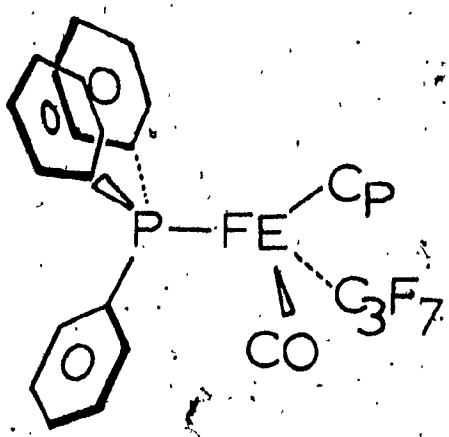

These two have the same I.R.

(1) and (2) are 'different' molecules; they are called diastereomers. Unfortunately, as only one peak is observed in the solid state (i.e., presumably only one diastereomer is present in the crystal), the crystal structure analyses are unlikely to confirm this.

SECTION II INTRODUCTION

PART (A) CHEMICAL

(1) : CHEMISTRY OF TRANSITION METAL-CARBON BOND

A transition metal can be linked to a carbon through a single electron-pair bond, or through a link possessing multiple bond character. The electron-pair metal carbon bond is analogous to that found in organo-derivatives of main group metals [e.g. $(CH_3)_4Pb$]. It is formed by overlap of two orbitals, each containing one electron, along the axis joining the two atoms. In molecular orbital terminology this is a σ bond. In the majority of known organo-transition metal compounds, however, current theory proposes multiplicity in bonds between the metal and the carbon atom. Thus in metal-carbon linkages in carbonyls, and perhaps in some cyanides, it is believed that there is not only a σ bond, involving donation of an electron pair in an sp orbital of carbon to a vacant orbital on the metal, but also a partial π bond. The latter can arise through overlap of a filled d or d-hybrid orbital of the metal and a vacant, or partially vacant, unhybridized p orbital of the carbon. Similarly, in the so-called 'π complexes' where unsaturated hydrocarbon molecules or ions donate π-electrons to form σ bonds to metal, π -bonding is believed to occur through overlap of filled metal d orbitals with vacant antibonding orbitals

on the hydrocarbon moieties. The π component of the bond plays an important role, because it provides a mechanism for removing electronic charge from the metal into bonding regions between the ligand and the metal, thereby strengthening the metal-carbon linkages. This strengthening by π bonding cannot operate between transition metals and the carbon atoms of alkyl groups because the latter have no low-energy vacant orbitals.

It is not surprising, therefore, that alkyl group-transition metal linkages are usually less stable than those between transition metals and π electron donors which possess the π^* antibonding orbitals. It is less obvious, however, why alkyls of transition metals should in general be less stable than those of the metals of the main groups of the Periodic Classification.

Many of the simple alkyl transition metal complexes exist only at low temperatures and some are also extremely sensitive to air and moisture. The latter property is also found with alkyl compounds of some metals of the main groups of Periodic Table (e.g. alkali metals), but is not found with organo-compounds of other metal such as Tin. Moreover, alkyl compounds of main group metals tend to be more stable thermally than their transition metal counterparts. Several suggestions have been put forward to account for these observations.

Jaffe and Doak[1] believe that normal σ bonds involving a carbon sp^3 orbital, and a suitable orbital on a transition metal, are weaker than those to main group metals because they have only about one-third of the ionic resonance energy which stabilizes alkali metal alkyls and only about half the covalent energy that leads to stable bonds to other main group elements.

Transition metal complexes containing alkyl and aryl groups σ bonded to the metals are found to have different stabilities. Several transition metal complexes have been prepared in which aryl groups are σ-bonded to the metals. They are often more stable than their alkyl analogs, and sometimes exist where the latter cannot be prepared. The enhanced stability could perhaps be due to the higher electronegativity of aryl groups compared with alkyl, leading to a larger ionic resonance energy in the carbon-metal σ bond, or to the possibility of π bonding between the metal's d electrons and vacant π^* orbitals. On the basis of the limited data available it would appear that σ bonds between aryl groups and transition metals are less robust than the bonds in comparable π complexes involving olefins, polyolefins, or aromatics.

Chatt and Shaw[2,3] proposed that the occurence of metal-carbon σ bonds is usually favored by the simultaneous presence on the metal of specific ligands, cyclopentadienyl groups, etc. These ligands are those which are believed to form π as well as σ bonds to transition metals. It was suggested that the effect

of this π bonding in the complex is to enhance the energy difference between the highest energy orbital which contains electrons and the lowest energy orbital which is vacant. π electrons bonding lowers the energy of the highest energy d orbital which contains electrons by involving these electrons in bonding. In this manner the energy required to promote the electrons into a vacant orbital of the complex as a prelude to decomposition is increased.

In this respect it is interesting to note that in the more stable organo-derivatives of the transition metals either the Sidgwick Effective Atomic Number Rule is obeyed, so that the metals have the closed shell configuration of the rare gases, or the number of electrons associated with the metals is two less than the rare gas configuration. In terms of ligand field theory this is predicted to give rise to relatively high ligand field stabilization. Unlike the situation with main group metals such as tin or lead, it is not possible to surround a transition metal with a sufficient number of alkyl or aryl groups to achieve a rare gas electron configuration. The σ bonded groups are only one-electron donors, considering the metal to be in the zero-valent state. Since transition metals lack anywhere up to eight ($Ni^0, 3d^8 4s^2$) electrons to attain their Effective Atomic Number it would be sterically impossible to achieve this goal solely with σ bonded groups.

b : BONDING IN METAL TO FLUOROALKYL DERIVATIVES

A review on fluorocarbon derivatives of metals[14] has been published by R.M.Treichel and F.G.A.Stone. The relative stability of metal-alkyl and fluoroalkyl complexes can be discussed from two points of view which are not necessarily mutally exclusive.
(1) : An essentially electrostatic model would imply that the bonding of the fluoroalkyl group to the metal may lead to considerable metal orbital contraction and a stronger carbon σ bond than for the case of equivalent alkyl complex. (2) : A second explanation is based on the possible π-acceptor properties of the fluoroalkyl group with respect to filled metal orbitals. In both these descriptions a shortening of the metal-carbon (fluoroalkyl) bond length compared with the metal-carbon (alkyl) value is expected. A more detailed description is as follows :

(i) : By applying the idea of Jaffe and Doak mentioned before, the metal-carbon bond should be expected to be more stable. This is because perfluoroalkyl groups are highly electron attracting, this will increase the electronegativity difference between the transition metals and the organic groups, consequently, it would raise the ionic resonance energy and thus stabilize the bonds.

(ii): In terms of the valence bond approach, the relatively great thermal and aerobic stability of transition metal fluoroalkyls

has been explained[5,6] as the result of resonance between such canonical forms as :

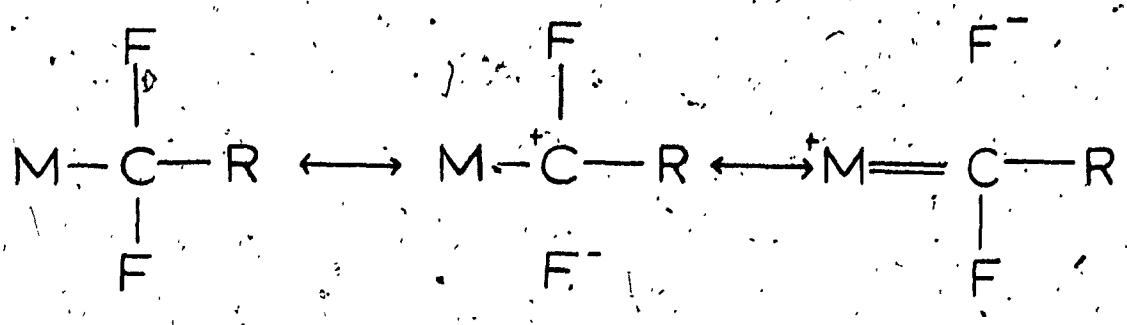

Cotton and McCleverty[7] suggested that the metal-fluoroalkyl linkage is strengthened as a result of $d\pi - \sigma^*$ back donation from the metal to the ligand. In the infrared spectra of some perfluoro-methyl compounds, the carbon-fluorine stretching modes of $CF_3Mn(CO)_5$ occur some 100 cm^{-1} lower than those in simple perfluoromethyl compounds such as CF_3Cl. This is interpreted as a result of electrons drifting from the $d\pi$ orbitals of appropriate (i.e., "quasi-E") symmetry.

M.Churchill has elucidated the crystal structure[6] of π-$C_5H_5Rh(CO)(C_2F_5)I$ to investigate the metal-carbon bond length. The perfluoroethyl group is in the expected staggered conformation, the Rh-C distance being 2.08 Å compared to the rhodium-carbonyl distance of 1.97 Å. Since the difference between the covalent radii of sp^3 and sp hybridized carbon atoms is 0.07 Å, the excess π character in the rhodium-carbonyl bond results in a decrease of only 0.04 Å relative to the rhodium-perfluoroethyl linkage. A similarly small difference is found for the Co-CF_2

and Co-CN bonds in $K_3[Co(CN_5)CF_2CF_2H]$ examined by R.Mason and D.R.Russell.[8] For transition metal (non-fluorinated) alkyls[9-11], however, the difference (Δ) in metal-carbon bond lengths for the alkyl and carbonyl groups is significantly greater (see Table 1).

These comparisons suggest that the rhodium perfluoroalkyl bond in π- $C_5H_5Rh(CO)(C_2H_5)I$ is considerably shorter than might be expected for a simple metal-carbon σ bond. However, evidence of bond shortening cannot differentiate between orbital contraction on the rhodium atom (due to high electronegativity[4] of the perfluoroethyl group) and the alternative of π donation from the metal $d\pi$ orbitals (in this case, $d_{xy}, d_{x^2-y^2}$) into C-F antibonding orbitals. Although the C_α- C_β bond length (1.57 ± 0.04 Å) is not significantly different from a simple single bond, angles around the α carbon of the perfluoroethyl do give some support for $d\pi$ -σ^* back donation. As back donation increases the double-bond character in the rhodium-perfluoroethyl linkage, the angles Rh-C_α-C_β , Rh-C_α-F_1, Rh-C_α-F_2 are expected to increase from the regular tetrahedral value (due to the increasing repulsion of the electrons in the Rh-C bond from those in the C_α -C_β , C_α -F_1, and C_α -F_2[12] bonds). Such distortions do, in fact, occur (Rh-C_α-C_β =116.4°, Rh-C_α -F_1 = 110.6°, Rh-C_α-F_2 =113.6°).

TABLE (1) : A COMPARISON OF METAL-CARBON BOND LENGTHS IN SOME TRANSITION METAL FLUOROALKYLS AND ALKYLS.

COMPLEX	BOND	d_{M-C} (with esd) Å	Δ** Å
π-$C_5H_5Rh(CO)(C_2F_5)I$ (6)	Rh-CF_2	2.08 (±0.03)	
	Rh-CO	1.8[illegible] (±0.03)	0.04
$K_3[Co(CN)_5CF_2CF_2H]$ (8)	Co-CF_2	1.990 (±0.014)	
	Co-CN(trans)	1.927 (±0.014)	(-)0.007
π-$C_5H_5Mo(CO)_3C_2H_5$ (9)	Mo-CH_2	2.38 (±0.03)	
	Mo-CO	1.97 (±0.03)	0.34
$(OC)_2Fe(\pi C_5H_4)$-$CH_2Fe^*(CO)_4$ (10)	Fe^*-CH_2	2.21[illegible] (±0.01[illegible])	
	Fe^*-CO(trans)	1.[illegible] (±0.01[illegible])	0.[illegible]
π-$C_5H_5Re(CH_3)_2C_5H_5CH_3$ (11)	Re-CH_3(av.)	2.2[illegible] (±0.03)	
	Re-CO	[illegible]2.00	[illegible]0.18

** Δ is the contraction of the metal-carbonyl (or cyanido) bond length relative to the metal-alkyl (or fluoroalkyl) distance after correction has been made for the different hybridization states of the carbon atoms.

Consistent results have been obtained by Mason and Russell in $K_3[Co(CN)_5CF_2CF_2H]$ which shows a $Co-C_\alpha-C_\beta$ angle of 119.7 ± 0.9°. Also, in π-$C_5H_5Mo(CO)_3C_3F_7$ studied by Churchill and Fennessey[65], $Mo-C_\alpha-C_\beta = 123.3°$.

It must be realized, however, that nonfluorinated transition metal alkyls also show $M-C_\alpha - C_\beta$ angles greater than the regular tetrahedral value.

(2) : BONDING IN (h-C_5H_5) METAL COMPOUNDS

The bonding between cyclopentadienyl and metal is best treated by the LCAO-MO approximation[13]. Taking ferrocene as an example, a semiquantitative energy diagram is given in FIG (2).

Each C_5H_5 ring, taken as a regular pentagon, has five π MO's, one strongly bonding (a), a degenerate pair which are weakly bonding (e_1), and a degenerate pair which are markedly antibonding (e_2), as shown in FIG (3).

The pair of rings taken together then has ten orbitals and, if D_{5d} symmetry is assumed, so that there is a center of symmetry in the $(h^5\text{-}C_5H_5)_2M$ molecule, there will be centro-symmetric (g) and antisymmetric (u) combinations. On the left of FIG.(2) is the original set of orbitals in the rings, and on the right are the valence shell (3d,4s,4p) orbitals of the iron atom. In the centre are the MO's formed when the ring π orbitals and the valence orbitals of the iron atom interact.

For ferrocene $(h^5\text{-}C_5H_5)_2Fe$, there are 18 electrons to be accomodated : five π electrons from each C_5H_5 ring and eight valence shell electrons from the iron atom. It will be seen that the pattern of MO's is such that there are exactly nine bonding MO's and ten antibonding ones. Hence the 18 electrons must

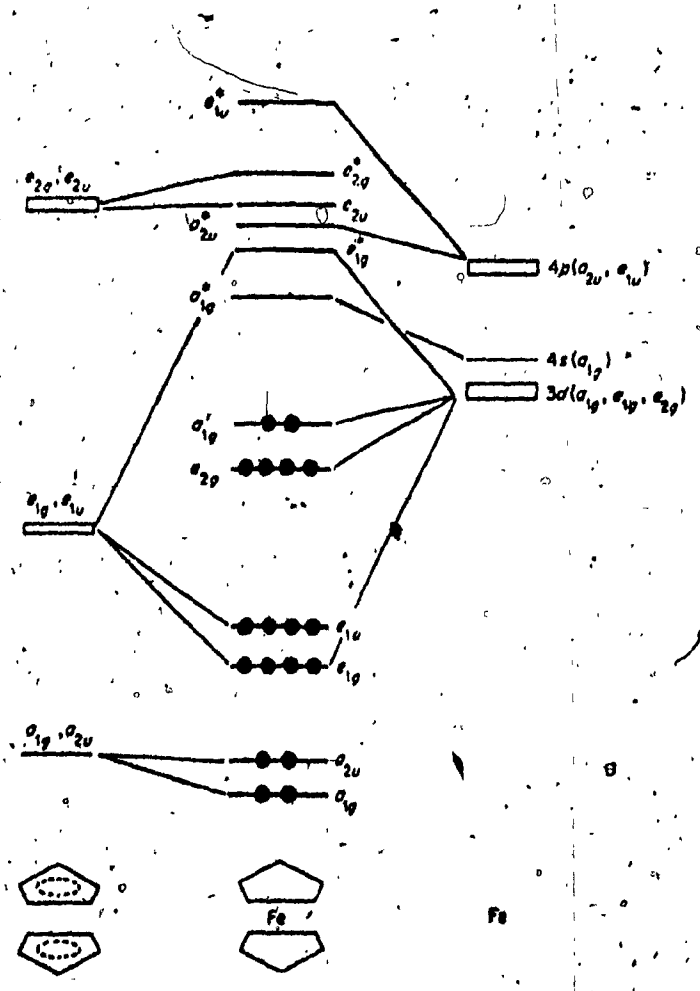

FIG (2). AN APPROXIMATE MO DIAGRAM FOR FERROCENE.

[a]Different workers often disagree about the exact order of the MO's; the order shown here, especially for the antibonding MO's, may be incorrect in detail, but the general pattern is widely accepted.(86)

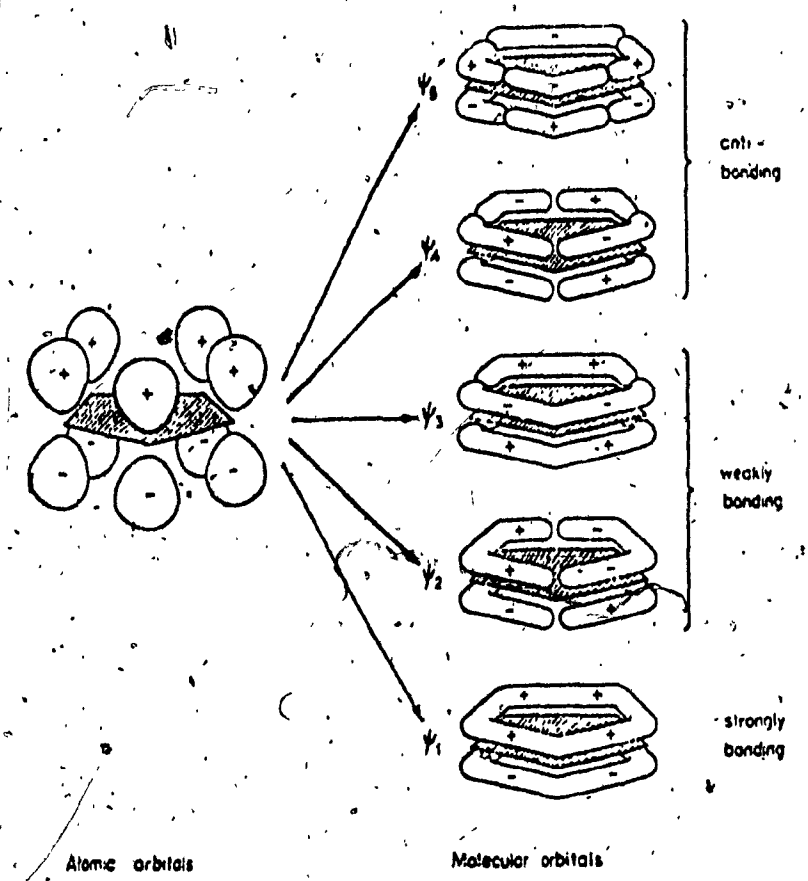

FIG. (3) THE π MOLECULAR ORBITALS FORMED FROM THE SET OF p_π ORBITALS OF THE C_5H_5 RING.

fill the bonding MO's, giving a closed configuration. Since the occupied orbitals are either of a type , which are each symmetric around the 5 fold molecular axis , or they are pairs of e_1 or e_2 type which are also, in pairs, symmetrical about the axis , no intrinsic barrier to internal rotation is predicted. The very low barriers observed may be attributed to van der Waals forces directly between the rings.

It can be seen in FIG.(2) that among the principal bonding interactions is that giving rise to the strongly bonding e_1g and strongly antibonding e_1g^* orbitals. In order to see the nature of this particularly important interaction more clearly, FIG.(4) shows how ring and metal orbitals overlap. This particular interaction is in general the most important single one because the directional properties of the e_1-typed d orbitals (d_{xy} and d_{yz}) give excellent overlap with the $e_1$type ring π orbitals.

(h^5-C_5H_5) Metal compounds can be considered either ionic or covalent compounds .

(1) . Ionic Compounds .

Cyclopentadiene is weakly acidic, dissociating to form H^+ and the pentagonal ion $C_5H_5^-$. With the cations of very electropositive metals, this ion forms essentially ionic compounds which may appropriately be called cyclopentadienides.

The principal ones are formed by the alkali metals, MC_5H_5, the alkaline-earth metals, $M(C_5H_5)_2$, the lanthanides and the actinides $M(C_5H_5)_3$. Europium gives $Eu(C_5H_5)_2$. In addition, $Mn(C_5H_5)_2$ also seems to be ionic, since the Mn(II) therein retains its spin sextuplet d^5 configuration, and the compound is strongly antiferromagnetic much like other ionic MnX_2 compounds. The ionic cyclopentadienides are typically very reactive toward air and water and react readily with ferrous chloride in tetrahydrofuran to give ferrocene.

(2) : Covalent Compounds :

It is also possible to have covalent $(h^5\text{-}C_5H_5)M$ groups even when the metal atom has no valence-shell d orbitals provided it has p orbitals of suitable energy and size. As shown in FIG.(5), a pair of p_x and p_y orbitals can overlap with the e_1 π orbitals of C_5H_5 in much the same way as do d_{xz} and d_{yz} orbitals. The C_5H_5In and C_5H_5Tl molecules are of this type of bonding.

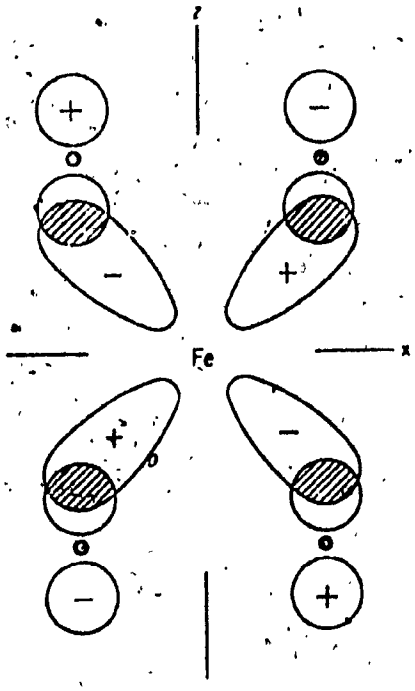

FIG. (4) A SKETCH SHOWING HOW ONE OF THE e_1 TYPE d ORBITALS, d_{xz} OVERLAPS WITH AN e_1 TYPE RING π ORBITAL TO GIVE A DELOCALIZED METAL–RING BOND. THE VIEW IS A CROSS SECTION TAKEN IN THE XZ PLANE.

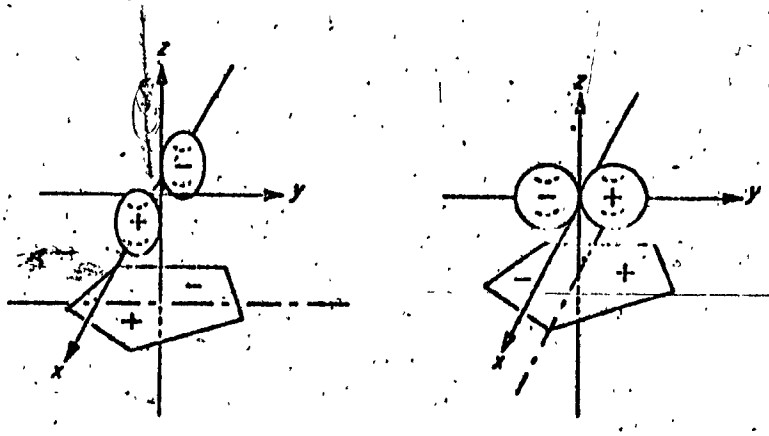

FIG. (5) DIAGRAMS SHOWING HOW P_x AND P_y ORBITALS ARE SYMMETRY-ADAPTED TO OVERLAP THE e_1 π ORBITALS OF A C_5H_5 RING.

(3) THE TRANSITION METAL-PHOSPHORUS BOND.

Transition metal complexes having phosphine ligands PX_3 are found to be stable[14,15]. The reason for this stabilising effect is that phosphine acts as a σ bond donor and a π-bond acceptor, the vacant 3d orbitals of the phosphorus being capable of interaction with filled nonbonding d orbitals of a transition metal. Thus back donation (shown in FIG.(6)) from a filled metal d orbital to an empty phosphorus 3d orbital in the PX_3 ligand can occur so strengthening the bond.

The extent to which back donation occurs depends on the electronegativity of the group X attached to the phosphorus atom. A more electronegative X leads to greater M $d\pi \rightarrow Pd\pi$ bonding. If this π bond is of greater importance than the σ bond, a strengthening and hence shortening of the $M-PX_3$ should result. If σ bonding is of importance, then increasing the electronegativity of X will lead to a weaker and longer M-P bond.

For example, structures of $Ph_3PCr(CO)_5$ and $(PhO)_3PCr(CO)_5$ have been determined[16]. The P-Cr bond in the latter compound

is 0.11 Å shorter than in the former. The Mdπ→ Pdπ bonding in such compound seems more significant then σ bonding.

Furthermore, the structure of π-$C_5H_5Fe[P(OC_6H_5)_3]_2I$.[17] shows a Fe-P bond length of 2.15Å. This bond is also markedly shorter than the Fe-P bond found in π-$C_5H_5Fe(CO)(\sigma$-$C_6H_5)P(C_5H_5)_3$; 2.24 Å[18]. This is due to the presence of more the electronegative element (O) in the former compound.

A similar shortening of the bond of the central atom with the phosphorus (or arsenic) is observed in many analogous complexes of the transition metals. In the molecule $(CO)_4Mn(H)[P(C_6H_5)_2]Mn(CO)_4$[19], the Mn-P distance of 2.28 Å is less than the sum of the tetrahedral radius of phosphorus (1.10 Å)[20] and the radius of Mn(1.39 Å)[21].

Of interest is the fact that the length of the M-P bond (M= Mn, Co,Ni) is practically independent of whether the P is a bridge or terminal atom. Examples of this are the structures $Mn(NO)(CO)_2[P(C_6H_5)_3]_2$[22], $Co[P(C_6H_5)_2H]_3Br_2$, and $Ni[P(C_6H_5)_2H]_3I_2$[23] in which the P atom is terminal , and on the other hand, the molecules $(CO)_4Mn(H)[P(C_6H_5)_2]Mn(CO)_4$[19] $[(C_6H_5)_2PCo(C_6H_5)]_2$ and $[(C_6H_5)_2PNi(C_6H_5)]_2$[24], where the P are bridge atoms.

The lengths of the metal-phosphorus bonds in these complexes are as follows:

$Mn-P_{terminal}$	2.28 Å	$Mn-P_{bridge}$	2.28 Å
$Co-P_{terminal}$	2.20 Å	$Co-P_{bridge}$	2.16 Å
$Ni-P_{terminal}$	2.18 Å	$Ni-P_{bridge}$	2.16 Å

In the complexes with arsine ligands, strengthening of the metal-arsinic bond is also observed. Thus, in the structure of mono-o-phenylene-bis-(dimethylarsine) iron tricarbonyl[25] the average Fe-As distance of 2.33 Å is considerably less than the sum of the covalent radii of the iron and arsenic atoms (2.50 Å)[20]. The multiple nature of the metal-Arsenic bond is also indicated by the Pt-As bond lengths (2.39 and 2.40 Å) in the complexes is $Pt\{C_6H_4[As(CH_3)_2]_2\}_2Cl_2$[26] and $Pd\{C_6H_4[As(CH_3)_2]_2\}_2I_2$[27] (the sums of the single bond covalent radii, according to the data of these authors are 2.49 and 2.52 Å respectively.)

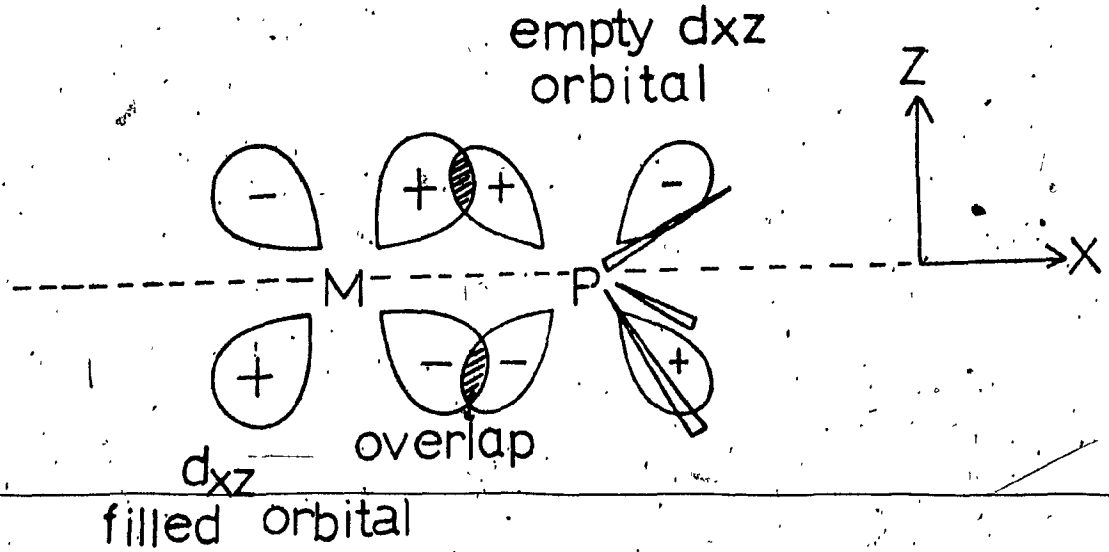

FIG.(6) DIAGRAM SHOWING THE BACK-BONDING FROM A FILLED METAL d ORBITAL TO AN EMPTY PHOSPHORUS 3d ORBITAL IN THE PX_3 LIGAND, TAKING THE INTERNUCLEAR AXIS AS THE x AXIS, AN EXACTLY SIMILAR OVERLAP OCCURS IN THE XY PLANE USING THE d_{xy} ORBITALS.

PART (B) : CRYSTALLOGRAPHIC

(1) : DIFFRACTION OF X-RAY BY CRYSTALS[28,29]

A crystal consists of atoms arranged in a pattern that repeats periodically in three dimensions. It is built from blocks of regularly repeated unit structures in space, and these units are stacked side by side in three dimensions. A lattice or grid system can be formed by drawing grid lines at equal intervals corresponding to the repeat distances of the structure; as a consequence, the surroundings of each grid-line intersection or lattice point, are identical.

In a three-dimensional lattice, the volume element or the parallelepiped whose edges are successive grid lines is termed a unit cell, which can generate the whole crystal by translating along the three edges, named a, b, and c. The angles between the axes are α, β, and γ, with α between b and c, β between a and c, and γ between a and b.

Since the repeated inter-atomic distances are of the same order of magnitude as X-ray wavelength (1 Å); it was suggested by Laue early in 1912[30], that the periodic structure as a crystal can be used to diffract x-rays.

In the same year, Bragg discovered that the diffraction process is analogous to the reflection of light by a plane mirror. Each grid constructed can act as a three-dimensional diffraction grating or reflection plane.

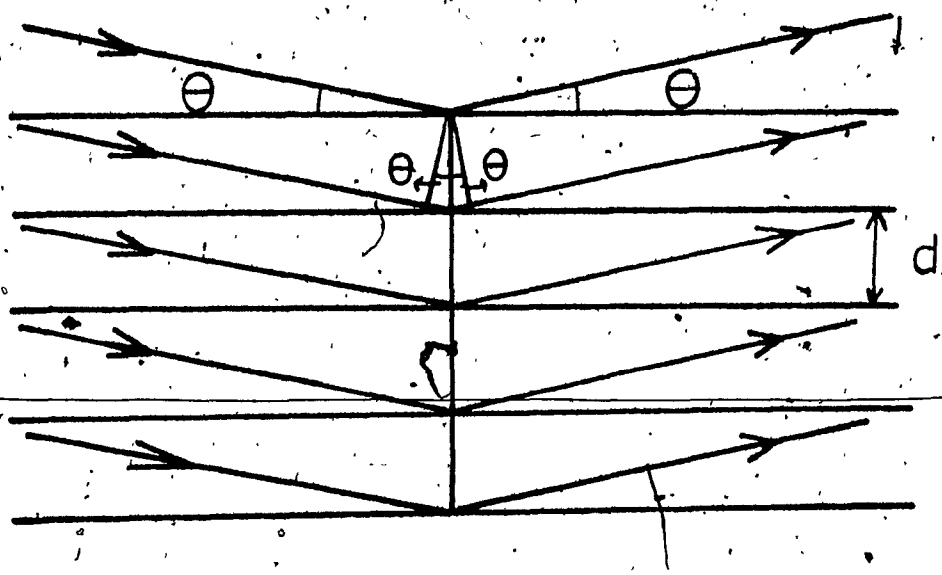

FIG(7)

construction showing conditions for diffraction

As shown in FIG (7), the diffraction angle 2θ, which is the angle between the incident and reflected beam directions is specified by the Bragg equation :

$$\theta = \sin^{-1} \frac{\lambda}{2d_{hkl}} \quad \text{.....(1)}$$

where λ is the wavelength of the x-radiation and d_{hkl} is the spacing of a set of planes (hkl) defined by the Miller indices, constructed through the points comprising the grid. The angle θ made by the incident beam equal the angle made by the diffracted beam at a stack of planes, hence, the diffracted beams are also termed reflections.

In order to visualize more clearly how diffraction occurs when the crystal is rotating along one of its axes, it is necessary to introduce the concept of the reciprocal lattice. The reciprocal lattice may be defined as follows : consider a normal to each possible direct lattice plane (hkl) to radiate from some lattice point taken as orgin and terminate each normal at a distance $1/d_{hkl}$ from this origin, where d_{hkl} is the perpendicular distance between planes of the set (hkl). The set of points so determined constitutes the reciprocal lattice (r.l.). The normal from the origin of the unit cell to the planes (1 0 0) (0 1 0) (0 0 1) at a distance 1/a, 1/b; 1/c, respectively will be the reciprocal axes a^*, b^*, c^*. By construction, a^* must be

perpendicular to the b c plane; similarly the b^*c^* plane of the r.l. must be perpendicular to the a direct axis.

Consider a crystal in a beam of x-rays of wavelength λ ; oriented in such a way that the x-ray beam is parallel to its a^*c^* plane; XO (FIG.8) is a line in the direction of the beam and passing through the r.l. origin O, Let C be a point on XO such that $CO = 1/\lambda$, then draw a circle with center C and radius CO. Suppose P, one of the r.l. points, lies on the circumference as in fig. (8), where

$$\sin\theta = \frac{OP}{2 \times 1/\lambda}$$

$$\therefore \sin\theta = \frac{OP}{2}\lambda \qquad \text{since } OP = 1/d_{hkl}$$

$$= \frac{1/d_{hkl}}{2} \times \lambda$$

$$\text{i.e.} \qquad 1\lambda = 2 . d . \sin\theta$$

This derivation implies that whenever a r.l. point coincides with a circle constructed as described, Bragg's law is satisfied and reflection occurs. The construction is not limited to the a^*c^* section, but will hold for all points on the sphere produced by rotating the circle about its diameter O B. By rotating the lattice about its origin, various r.l. points can be brought into coincidence with the surface of the sphere of reflection and the

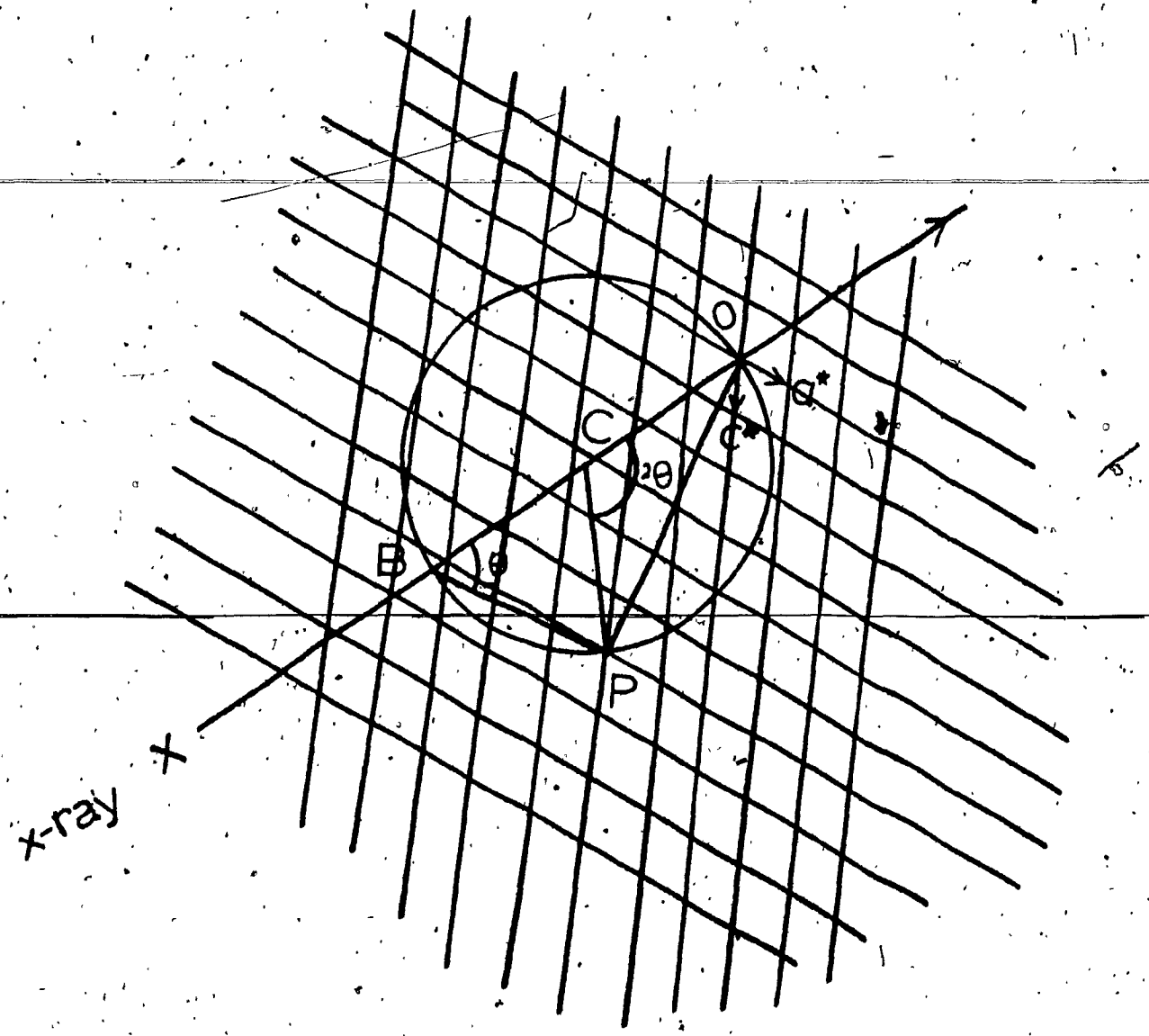

FIG (8)
THE RECIPROCAL LATTICE AND THE SPHERE OF REFLECTION

corresponding reflection observed.

If the crystal is oriented so that the xray beam is perpendicular to a direct lattice axis, since levels of r.l. points are normal to this axis, it is evident that rotation about the axis will cause each level of points to intersect the sphere in a circle. The diffracted rays will pass from the center of the sphere, through these circles forming cones, the zero level being a flat cone. The cone axes are coincident and parallel to the rotation axis. If the reflection sphere is surrounded by a film, then the reflection can be met. (see FIG.(9))

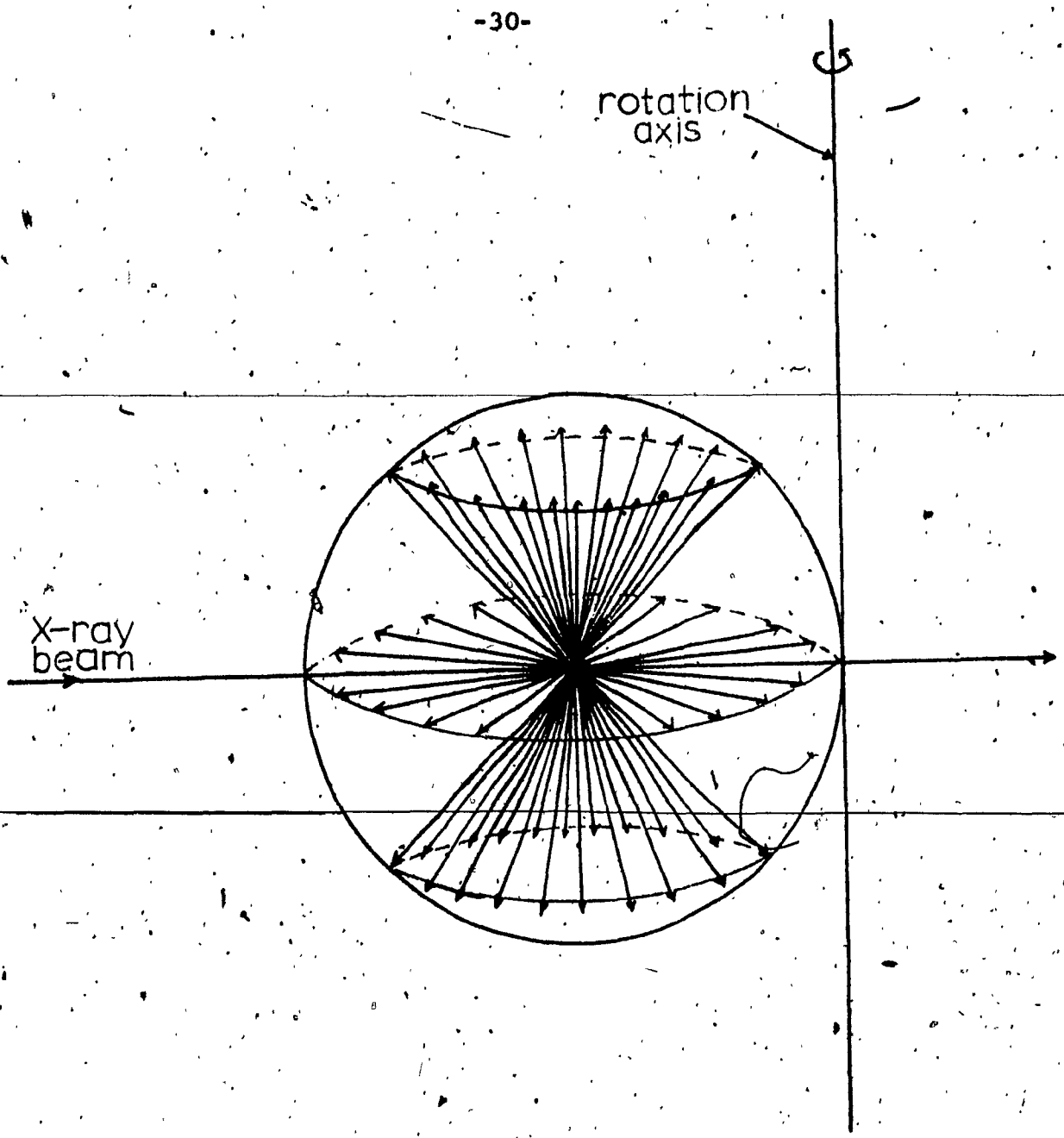

FIG (9)

(2) : SPACE GROUP DETERMINATION

To investigate the crystallographic diffraction data, first some photographic work is done to determine the cell constants and space group. A Weissenberg photograph[31] is a rotation photograph of about 180° with a cylindrical metal screen that allows only one layer line at a time to reach the film.

The film is shaped into a cylinder around the sphere of reflection and parallel to the axis of crystal rotation, the distance of a spot from the center line is proportional to the angle 2θ of the diffracted beam. The camera is designed so that 1 m m. in the 2θ direction on the unrolled film is equal to 2° in 2θ. Also, since the film is moved past the slot in the layer screen back and forth at a constant rate while the crystal is being rotated uniformly, the position of the spots in the direction along the central line of the film will be proportional to the crystal rotation. Thus, a Weissenberg diffraction photograph can record only one layer of reflections, i.e., if the crystal is oriented about the a axis, then a layer of (o,k,ℓ) or $(1,k,\ell)$ etc. can be obtained. Since a Weissenberg photo can supply information only on planes perpendicular to the rotating axis, in order to obtain more information on the

other planes without remounting the crystal along the other axis, a precession camera is best used.

The precession camera was designed by Buerger[32] in the 1940s. It is a moving crystal, moving film device for mapping one reciprocal lattice level onto one sheet giving an undistorted record of diffraction spots from which the angles, and distances of the lattice, may be read off.

The precession theory is as follows : consider a direct lattice axis which is parallel to the incident beam, the zero level r.l. net which is perpendicular to it is thus tangent to the sphere of reflection at the origin as shown in FIG. (10 a). If the crystal is rotated through a small angle $\bar{\mu}$ about an axis perpendicular to the beam, then the r.l. net will cut the sphere which passes through the origin O as is illustrated in FIG.(10 b).

If the crystal is moved in such a way that the direct axis AO revolves about the beam, keeping the constant angular separation $\bar{\mu}$, the intercepted circle will revolve about the origin in the r.l. plane; the diffracted rays, passing from the center of the sphere through the points on the circle, will project an undistorted image of their relationship onto the film as in FIG.(10 c).

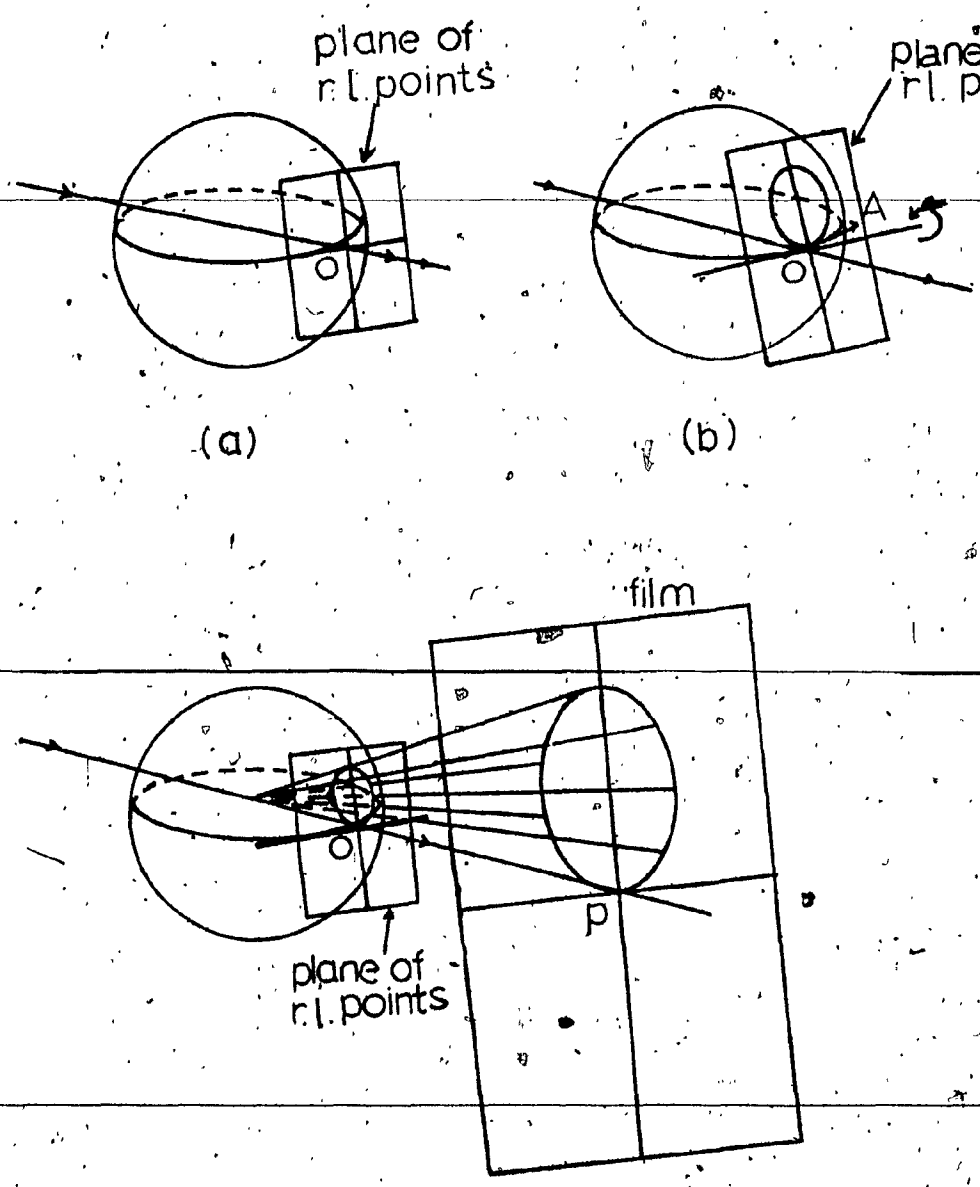
plane of
r.l. points
O
(a)
plane of
r.l. points
A
O
(b)
film
O
P
plane of
r.l. points
(C)

FIG(10)

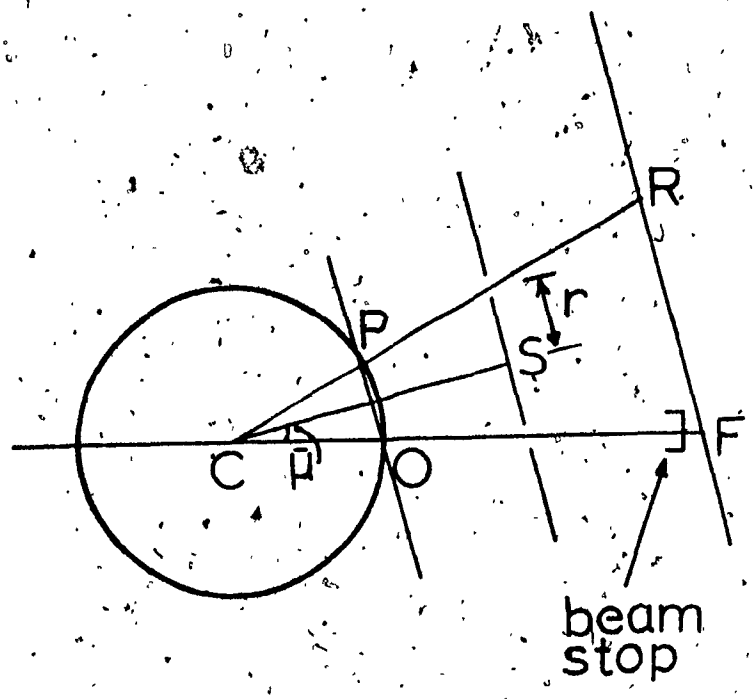

FIG(11)

Since it is not only the zero-level r.l. net that will pass through the sphere and cause reflections , it is necessary to use a screen to isolate the reflections of the reciprocal net desired. The screen is placed parallel to the film , between the film and the crystal. The arrangement is such that the cone of diffracted rays from the plane of interest will pass through the clear ring on its way to the film. As the crystal moves, the level screen precesses to keep the normal through its center coincident with that through the center of the reflecting circle. In this way, the arrangement as shown by FIG ,(11) is maintained while the crystal axis revolves about the beam.

The film to crystal distance is usually 60.0 m m. for zero level photographs, the film being advanced toward the crystal for recording upper levels. The maximum value of $\bar{\mu}$ is 30°.

The relationship of reciprocal lattice space and precession geometry is thus shown by FIG.(12).

By using the Weissenberg and precession photographs to complement each other, the presence of symmetry and the systematic absences can be determined, and thus the space group can be deduced.(33)

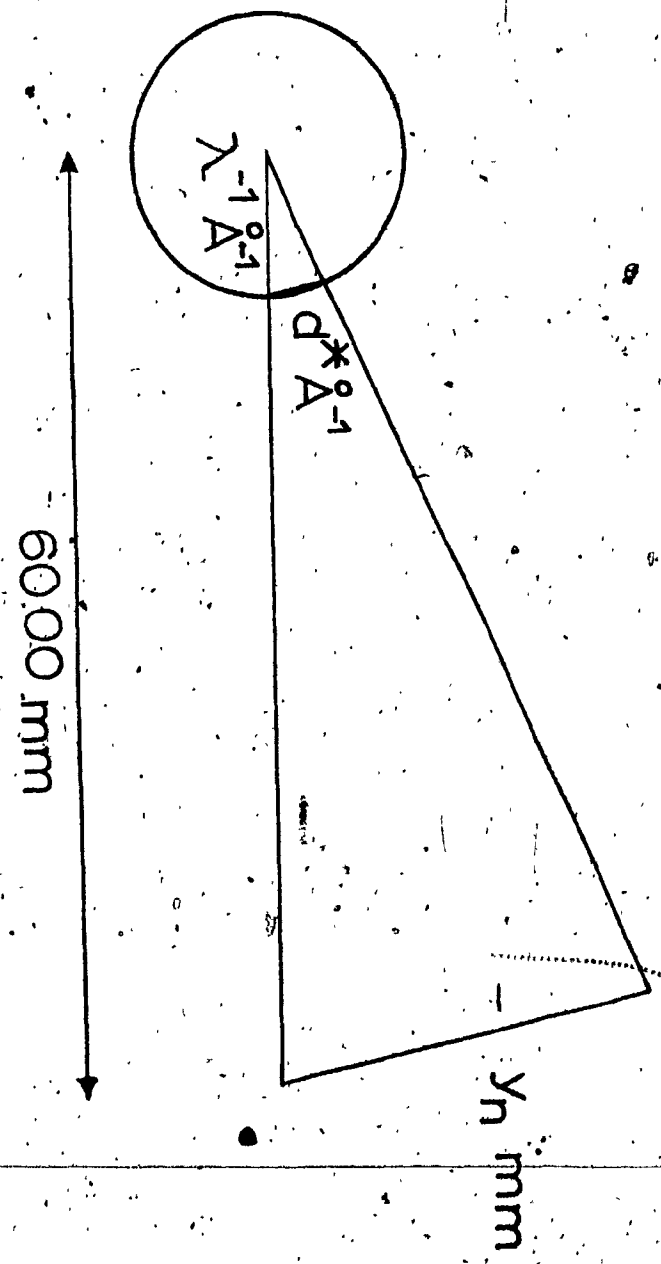

FIG(12)

(3) : DATA COLLECTION

The reason for collecting the intensities of the reflections is that from these data, one may deduce the electron-density distribution in the crystal-cell. The intensity of a reflection is defined as : "a measure of the total number of photons of the characteristic wavelength being used which are diffracted in the proper direction by a reciprocal lattice point passing from the outside to the inside of the sphere of reflection or vice versa."

Ideal intensities defined as above are impossible[34,35] to collect since they always accompanied by a certain amount of other scattered radiation (background)arising from different sources, e.g. the diffuse scattering of x-rays of all wavelengths by all objects in the beam, including air and the crystal. A more serious problem arises from the non-monochromaticity of the x-ray beam due to the K_β line and the separation of $K_{\alpha 1}$ and $K_{\alpha 2}$.

The amount of data available for any crystal is limited by the wavelength of the radiation used since the radius of the reflection sphere is equal to $1/\lambda$. There is a more practical limit because intensity becomes very low at angles above $45 = 2\theta$ using MoK_α radiation. Because of symmetry of the reciprocal lattice, those reflections having indices related in certain ways will have the same intensities, so only one portion cut from

the sphere (a hemisphere or less) need usually be measured.

A four-circle diffractometer is used to collect the intensity data and a scintillation detector with a pulse-height analyser[36] is currently used for the measuring of intensity. The diffractometer has four angles ($2\theta, \omega, \chi, \phi$) which may be used to set up the orientation of the crystal so as to bring any desired plane into the reflecting position. The detector is mounted on the 2θ circle, the χ and ϕ arcs are used to bring any desired r.l. point into contact with the sphere of reflection in the plane defined by the source, crystal and detector (i.e. the zero level weissenberg position). The ω scan may be used to carry a lattice point of the central line of the film on a zero-level Weissenberg from outside of the sphere of reflection to the inside. A 2θ scan will pass through reflections on a common central row.

In setting up the orientation of the crystal in the diffractometer for the data collection, a minimum of 3 reflections are required. Two reflections can be measured approximately from the Weissenberg zero level. From the zero level Weissenberg photograph, a strong reflection is chosen. Its measured 2θ angle is set on the diffractometer (1 m m. from central line $\simeq 2^\circ$), then ω, χ, and ϕ are set to zero, and ϕ scanned until the reflection chosen is located. (ω is parallel to ϕ but is not used because a collision will occur.) Scanning 2θ at this predetermined ϕ value could confirm the axial diffraction intensity pattern. Another reflection chosen from the

zero level Weissenberg can also be found using this method. The position of the third reflection can be predicted by using the 2 reflections already found (and centered) plus the "film measured" unit cell parameters; or, if there is a reciprocal axis parallel to ϕ, then with $\chi = 90^\circ$, a reflection on the third axis can be found. Centering of these reflections allows calculation of an initial orientation matrix. Twelve more reflections are centred, which are chosen with sufficiently high 2θ values and positions covering the reciprocal lattice reflections evenly and completely. To ensure that the crystal is oriented properly, a least squares refinement is done at this stage. The input parameters to the least squares refinement are the six approximate cell constants and ω, χ, and ϕ for a primary and a secondary reflection (chosen such that their χ angles are close to 0° and their ϕ angles are separated by about 90°). The following are refined : the variable cell parameters, ω and χ of the primary reflections and χ of the secondary refection. The estimated standard deviations of the cell parameters quoted are computed as a result of this least squares refinement. The refined ω and χ values of the primary and secondary reflections are used to compute an orientation matrix for the crystal which is then used for data collection.

The reflections comprising the three reciprocal unit cell axes are measured before data collection is started. Their intensities are compared to those measured after data-collection to ensure the stability of the crystal and of the instrument. The θ- 2θ scanning method is used to record the integrated intensity of the reflections. The crystal is moved slowly (1° per minute) so that the reflection being measured passes through the sphere of reflection in its equatorial plane. The length of the scan, specified for low angle reflections is determined. This varies according to the mosacity of the crystal examined and the value of 2θ . At high values of $\sin\theta / \lambda$, the separation between α_1 and α_2 diffraction is more pronounced than at low angles. To allow for this α_1-α_2 splitting a dispersion factor for MoK_α radiation is be used by the Picker Nuclear data collection program to compute the actual angular scan length for every reflection.

(4) : DATA REDUCTION

The intensity data so collected is just the raw data. In order to extract the correct observed intensity, it is necessary to do the following corrections :

(1) : Removal of background intensity :

The reflection intensity I can be obtained from the equation :

$$I = N - [B_1 + B_2](t_s / 2 t_b) \quad \ldots\ldots\ldots(2)$$

where N is the peak count in the scan time t_s seconds, B_1 and B_2 are the background counts on either side of the peak, each measured for t_b seconds. If I is computed to be less than 0.0, the reflection is considered absent. The standard deviation σ (I) of the intensity I is calculated by :

$$\sigma(I) \quad [N + \frac{(B_1 + B_2)}{2} \quad (\frac{t_B}{t_b})^2 + (0.02N)^2]^{1/2}$$

$$\ldots\ldots\ldots\ldots(3)$$

If the intensity I is less than 3σ (I), the reflection is considered as useless based on counting errors. Along with the absent reflections, these reflections will be rejected and used neither for structure solution nor for refinement.

(2) : Lorentz correction :

The Lorentz correction arises because the time required for a r.l. point to pass through the sphere of reflection varies with its position in reciprocal space and the direction it approaches the sphere. It depends on the precise measurement technique used.

$$L = \frac{\sin\theta}{\sin 2\theta \sqrt{\sin^2\theta - \sin^2\mu}} \quad \ldots\ldots\ldots(4)$$

where μ = equi-inclination setting angle for Weissenberg geometry. Then , for "zero level" reflections as measured on the diffractometer,

$$L = \frac{1}{\sin 2\theta} \quad \ldots\ldots\ldots\ldots(5)$$

(3) : Polarization correction

Polarization of the x-ray beam decreases the intensity of the diffracted (reflected) x- ray. This effect is dependent only on the diffraction angle; thus, observed intensities must be multiplied by 1/P where

$$1 / P = \frac{(\cos^2 2\theta_m + 1)}{(\cos^2 2\theta_m + \cos^2 2\theta_s)} \quad \ldots\ldots\ldots(6)$$

Correction for (2) and (3) can be applied simultaneously using a computer; a combined L_p, which is specific to the diffractometer geometry used is defined as :

$$L_p = \frac{(\cos^2 2\theta_m + \cos^2 2\theta_s)}{\sin 2\theta_s (\cos^2 2\theta_m + 1)} \quad \ldots\ldots\ldots(7)$$

where θ_s and θ_m are the diffraction angles at the sample crystal and monochromator crystal respectively.

The quantity required to derive the crystal structure is what is called the structure factor, F, which is related to the observed intensity by $F \propto \sqrt{I}$.[37] (It can be calculated theoretically from the position of the atoms in the cell when they are known.) Thus, taking the above corrections in account,[38,39]

$$|F_{hkl}| = \sqrt{I_{hkl} / L_p} \quad \ldots\ldots\ldots\ldots (8)$$

After data reduction, the numbers obtained are F relative's (F_{rel}) are obtained :

$$|F_{rel}| = K' |F_o| = \sqrt{I_{hkl} / L_p} \quad \ldots (9)$$

(4) : Absorption Correction [40-42]

This effect arises from the proportion of the incident and diffracted beams absorbed by the crystal. It depends on the path length through the crystal and on the material of which the crystal is composed. Correction can be made by calculating the absorption for the actual path length travelled within the crystal, by the beam reflecting from each infinitesimal portion of the crystal, and then integrating these results over the entire volume of the crystal.

(5) : INTENSITY STATISTICS

Once the corrections have been made, the output data is ready to use. The major function of this data is to compare it with the theoretically calculated structure factors based on the assumed arrangement of atoms.

The x-ray scattering power[43] for each kind of atom in the cell, f_o, is a function only of the atom type and $\sin\theta/\lambda$. At $\sin\theta/\lambda = 0$, it is equal to the total number of electrons in the atoms, while, as $\sin\theta/\lambda$ increases, the scattering factor decreases : this variation of scattering factor is a consequence of the finite size of the stationary atom. However, the electron distribution in an atom will not be in stationary state, it will vibrate about a mean position. The magnitude of the vibration depends on the temperature[44] and the mass of the atom. The effect of such thermal motion is to spread the electron cloud over a larger volume and thus reduce the scattering power (f) of a real atom :

$$f = f_o\, e^{-B(\sin^2\theta)/\lambda^2} \qquad \ldots\ldots\ldots\ldots(10)$$

where the thermal parameter $B = 8\pi^2\bar{\mu}^2$

$\bar{\mu}$ is the mean-square amplitude of atomic vibration.

This is the so-called isotropic case where the vibration is spherical and B is called the isothermal parameter.

In the anisotropic case, the thermal parameter is replaced by six parameters which describe the amplitude and orientation of vibration as an ellipsoid :

$$f = f_o \, e^{-(\beta_{11}h^2 + \beta_{22}k^2 + \beta_{33}l^2 + 2\beta_{12}hk + 2\beta_{13}hl + 2\beta_{23}kl)} \quad \ldots(11)$$

Finally, in order to compensate for the fact that the electrons are not free in the molecules but are bound, The free electron scattering factor f_j must be corrected by a real $\Delta f'$ (usually negative) and an imaginary $i\Delta f''$ dispersion correction. This correction is only significant for 'heavy' atoms.

Since $\bar{I}_{rel} = \langle F_{rel}^{\ 2} \rangle_{av}$

where I_{rel} is an average observed corrected intensity, the theoretical average intensity I_{abs} is equal to $\sum_{i=1}^{n} f_i^2$ where N is the number of atoms contained in a unit cell.

i.e.,

$$\bar{I}_{abs} = \sum_{i=1}^{N} f_{ei}^{\ 2} \, e^{-2B(\sin^2\theta)/\lambda^2} \quad \ldots\ldots(12)$$

$$= e^{-2B(\sin^2\theta)/\lambda^2} \sum_{i=1}^{N} f_{ei}^{\ 2} \quad \ldots\ldots(13)$$

If $\bar{I}_{rel} = c\,\bar{I}_{abs}$

$$\bar{I}_{rel} = c \, e^{-2B(\sin^2\theta/\lambda^2)} \sum_{i=1}^{N} f_{ei}^{\ 2} \quad \ldots\ldots(14)$$

$$\frac{\bar{I}_{rel}}{\sum_{i=1}^{N} f_{ei}^{\ 2}} = c \, e^{-2B(\sin^2\theta/\lambda^2)} \quad \ldots\ldots(15)$$

taking the natural logarithm of both sides,

$$\ln\left(\frac{\bar{I}_{rel}}{\sum_{i=1}^{n} f_{ei}^{\ 2}}\right) = \ln C - 2B\,(\sin^2\theta/\lambda^2) \quad \ldots\ldots(16)$$

If $\ln\left(\frac{\bar{I}_{rel}}{\sum_{i=1}^{N} f_{ei}^{2}}\right)$ is plotted against $\sin^2\theta/\lambda^2$,

the result should be a straight line where the intercept at

$(\sin^2\theta/\lambda^2) = 0$, is $\ln C$, and the slope is $-2B$.

If $= K\ \bar{I}/\sqrt{C}$, then $|F_{abs}| = K\,|F_{rel}|$.

This is known as a Wilson Plot, after A.J.C. Wilson.(45)

(6) : STRUCTURE FACTOR CALCULATION AND THE PHASE PROBLEM

Let $\rho(x,y,z)$ represent the electron density or number of electrons per unit volume near the point in the unit cell that has coordinate x,y,z.

The Fourier expansion ρ is :

$$\rho(x,y,z) = \frac{1}{V} \sum_h \sum_k \sum_l F_{hkl}\, e^{-2\pi i(hx+ky+lz)} \quad \ldots\ldots(17)$$

where F_{hkl} is the structure factor[59-61] whose amplitude is determined both by the scattering factors for the individual atom and by their phase δ . The phase is determined by the fractional co-ordinates of the atoms contributing to the reflection. The unit phase difference being 2π, thus.

$$\delta = 2\pi\ (hx + ky + lz\ )$$

The structure factor is expressed by :

$$F\ (hkl) = \sum_j f_j\, e^{2\pi(hx_j + ky_j + lz_k)}$$

$$= \sum_j f_j \cos 2\pi\ (hx_i + ky_j + lz_k\ ) + i \sum f_j \sin 2\pi(hx_j+ky_j+lz_k)$$

$$= A + i\ B \quad \ldots\ldots\ldots\ldots(18)$$

and $|F(hkl)|^2 = A^2 + B^2 \quad \ldots\ldots\ldots\ldots(19)$

Unfortunately, the information from the intensity data is proportional to F_{hkl}^2 but not F, so the sign (phase) for F is still not determined.

The phase angle associated with the structure factor is given by :

$$\phi = \tan^{-1} \frac{B_{hkl}}{A_{hkl}} \quad \text{.....(20)}$$

Since the phase angle is not known from the observed data, equation (18) cannot be solved for (x_j, y_j, z_j).

For a centrosymmetric structure, $x,y,z \equiv \bar{x},\bar{y},\bar{z}$ and equation (18) becomes :

$$F_{hkl} = A_{hkl} + i.o$$

where $A_{hkl} = 2 \sum f_j \cos 2\pi (hx_j + ky_j + lz_j)$.

The phase angle is 0 or π and the structure factor requires only a sign to be determined in order to solve equation (18).

The fundamental problem in crystallography is the determination of the phase angles, or for a centrosymmetric structure, the sign associated with each structure factor. This can only be done by determining the position, of some of the molecule in the unit cell. Then it is possible to calculate approximate Fourier Synthesis of $\rho(x,y,z)$, which will show the position of some or all of the rest of the atoms.

(7) : PATTERSON SYNTHESIS (46-48)

If the molecule contains a single atom heavier than the rest, it is possible to find out the position of heavy atoms approximately from a Patterson map.

A Patterson map is produced by the function :

$$P(u,v,w) = \frac{2}{V} \sum_{h} \sum_{k} \sum_{l} |F_{hkl}|^2 \cos 2\pi (hu + kv + lw) \quad \ldots\ldots\ldots\ldots (21)$$

thus, the coefficients used in the Fourier summation are the squares of the observed structure factors, so there are no phases involved. The peaks P (u,v,w) in a Patterson synthesis correspond to interatomic vectors. The information is used to solve for the positions of the heavy atoms in the cell. The largest peak (normalized to 999) is observed at the origin. There should be N^2-N vectors not on the origin (where N is the number of atoms in the cell). There is considerable overlap of peaks due to the diffuse character of the atom in space. This is minimized by the so called 'sharpened Patterson function'. The scattering power of the atom is corrected for the thermal motion and for its dependence on $\sin\theta/\lambda$. The squares of the sharpened structure factors are calculated from the squares of their observed structure factors by using :

$$\left(F_{sharp} \right)_{hkl}^{2} = \frac{[\ 0.1667 + (\sin^2\theta / \lambda)^2\ ]\ [F_{obs}]^2_{hkl}}{[\ \sum_{j=1}^{n} f_{\theta j}\ ]^2\ e^{-B(\sin^2\theta)/\lambda^2}} \qquad \ldots\ldots\ldots\ldots\ldots\ldots\ldots\ldots (22)$$

where B is the overall thermal parameter (usually about 1.5 to 2) and f_{θ_j} is the mean atomic scattering factor for the j^{th} atom. These squared structure factors so obtained are used in the Patterson synthesis.

The intensity of a Patterson peak resulting from the vector between two atoms of atomic numbers Z_1 and Z_2 is 999 times the ratio $Z_1 Z_2 / \sum_{j=1}^{n} Z_j$ where N is the number of atoms in the unit cell. Peaks due to vectors between symmetry related atoms enable the positions of these atoms to be fixed in relation to the symmetry elements concerned. Such peaks have one or more co-ordinates fixed by the nature of the symmetry operation and they are found on 'Harker sections' and 'Harker lines ' in a Patterson synthesis.

Thus, a Patterson synthesis yields approximate positional parameters for "Heavy " atoms and these may be used together with the vibrational parameters to calculate phases for $|F_{hkl}|$, possibly after some refinement.

(8) : LEAST SQUARES REFINEMENT OF ATOMIC PARAMETERS[49]

For higher accuracy, the best set of atomic parameters for calculation of phases may be obtained be minimizing the differences between observed $|F_o|$ and calculated $|F_c|$ structure amplitudes.

The quantity to be minimized is :

$$D = \sum_{hkl} W_{hkl} \left(|F_o| - |kF_c| \right)^2 \quad \ldots\ldots\ldots(23)$$

$$\sum_{hkl} W_{hkl} \left[|F_o| - |kF_c (p_1\ p_2\ \ldots\ldots\ldots p_n)| \right] \frac{\partial |kF_c(p_1 \ldots p_n)|}{\partial p_j} = 0$$

$$(j = 1,2,3,\ldots\ldots n) \ldots\ldots(24)$$

Since the structure factor is not a linear function, it must be approximated by expressing $|F_c|$ as Taylor series and neglecting second and higher powers,

$$|kF_c(p_1\ p_2 \ldots\ldots p_n)| = |kF_c\ (a_1 \ldots\ldots a_n)| + \frac{\partial |kF_c|}{\partial p_1} \Delta p_1 + \ldots\ldots + \frac{\partial |kF_c|}{\partial p_n} \Delta p_n$$

$$\ldots\ldots\ldots\ldots\ldots\ldots(25)$$

where $p_1 \ldots\ldots p_n$ may be the scale, positional and thermal parameters after improvement. Thus :

$$\Delta p_j = p_j - a_j$$

where the a_j are approximate " trial parameters "

Substituting equation (25) in (24) :

$$\sum_{hkl} W_{hkl} \left(|F_o| - |k\,F_c\,(a_1 \ldots\ldots a_n)| - \frac{\partial |k\,F_c|}{\partial p_1}\Delta p_1 - \ldots\ldots - \frac{\partial |kF_c|}{\partial p_n}\Delta p_n\right)\frac{\partial |kF_c|}{\partial p_j} = 0$$

$$(j = 1, 2, \ldots\ldots n) \ldots\ldots (26)$$

or

$$\sum_{hkl} W_{hkl} \left(\Delta F - \frac{\partial |kF_c|}{\partial p_1}\Delta p_1 - \ldots\ldots - \frac{\partial |kF_c|}{\partial p_n}\Delta p_n\right)\frac{\partial |kF_c|}{\partial p_j} = 0$$

$$(j = 1, 2, \ldots\ldots n) \ldots\ldots (27)$$

By expansion and rearrangement of (27), the following set of equations can be obtained :

$$\left\{\begin{array}{l}
\sum_{r=1}^{m} W_r \left(\frac{\partial |kF_{cr}|}{\partial p_1}\right)^2 \Delta p_1 + \sum W_r \frac{\partial |kF_{cr}|}{\partial p_1}\frac{\partial |kF_{cr}|}{\partial p_2}\Delta p_2 + \ldots\ldots \sum W_r \frac{\partial |kF_{cr}|}{\partial p_1}\frac{\partial |kF_{cr}|}{\partial p_n}\Delta p_n \\
\qquad = \sum_{r=1}^{m} W_r \Delta F_r \frac{\partial |kF_{cr}|}{\partial p_1} \\
\sum_{r=1}^{m} W_r \frac{\partial |kF_{cr}|}{\partial p_2}\frac{\partial |kF_{cr}|}{\partial p_1}\Delta p_1 + \sum_{r=1}^{m} W_r \left(\frac{\partial |kF_{cr}|}{\partial p_2}\right)^2 \Delta p_2 + \ldots\ldots \sum_{r=1}^{m} W_r \frac{\partial |kF_{cr}|}{\partial p_2}\frac{\partial |kF_{cr}|}{\partial p_n}\Delta p_n \\
\qquad = \sum_{r=1}^{m} W_r \Delta F_r \frac{\partial |kF_{cr}|}{\partial p_2} \\
\qquad \vdots \\
\sum_{r=1}^{m} W_r \frac{\partial |kF_{cr}|}{\partial p_n}\frac{\partial |kF_{cr}|}{\partial p_1}\Delta p_1 + \sum_{r=1}^{m} W_r \frac{\partial |kF_{cr}|}{\partial p_n}\frac{\partial |kF_{cr}|}{\partial p_2}\Delta p_2 + \ldots\ldots \sum_{r=1}^{m} W_r \frac{\partial |kF_{cr}|}{\partial p_n}\Delta p_n \\
\qquad = \sum_{r=1}^{m} W_r \Delta F_r \frac{|kF_{cr}|}{p_n}
\end{array}\right. \quad \ldots\ldots (28)$$

The above system of n equations in n unknowns, the Δp_j's, are linear and can be solved conveniently by matrix methods as follows : the normal equations(28) may be written as

$$\left.\begin{aligned} a_{11}X_1 + a_{12}X_2 + \ldots\ldots + a_{1n}X_n &= V_1 \\ a_{21}X_1 + a_{22}X_2 + \ldots\ldots + a_{2n}X_n &= V_2 \\ \vdots \\ a_{n1}X_1 + a_{n2}X_2 + \ldots\ldots + a_{nn}X_n &= V_n \end{aligned}\right\} \quad \ldots\ldots(29)$$

Where $a_{ij} = \sum_{r=1}^{m} W_r \frac{\partial |F_{cr}|}{\partial p_i} \frac{\partial |F_{cr}|}{\partial p_j}$; $x_j = \Delta p_j$, $V_i = \sum_{r=1}^{m} W_r (F_r) \frac{\partial |F_{cr}|}{\partial p_i}$,

in matrix form :

$$\begin{pmatrix} a_{11} & a_{12} & \ldots\ldots\ldots & a_{1n} \\ a_{21} & a_{22} & \ldots\ldots\ldots & a_{2n} \\ \vdots & \vdots & & \vdots \\ a_{n1} & a_{n2} & \ldots\ldots\ldots & a_{nn} \end{pmatrix} \begin{pmatrix} X_1 \\ X_2 \\ \\ X_n \end{pmatrix} = \begin{pmatrix} V_1 \\ V_2 \\ \\ V_n \end{pmatrix} \quad \ldots\ldots(30)$$

or,

$$A\,X = V \quad \ldots\ldots\ldots\ldots(31)$$

thus, $X = A^{-1}\,V$

The computer program SFLS can separate the matrix into several matrices (up to 9 in number). ΔP_j's are obtained and the new parameters can be used in calculating improved structure factors.

The Least Squares calculation must be repeated using approximate values derived from the preceding calculation. The process is complete when there is no significant change in the parameters between two successive cycles.

If W_{hkl} is the weight of ΔF_{hkl} (which is set equal to the reciprocal of sigma), the estimated standard deviation of parameters (p_j) can be obtained from :

$$\sigma(p_j) = \sqrt{b_{jj} \left[\sum_{hkl} W_{hkl} \Delta F_{hkl}^2 \right] / (m-n)} \qquad \ldots\ldots\ldots\ldots\ldots\ldots (32)$$

where m is the number of observations, n is the number of parameters. b_{jj} is the diagonal element of the inverse matrix.

The discrepancy index R is the residual or 'reliability factor' which can be computed from :

$$R = \frac{\sum_{hkl} \left| |F_{obs}|_{hkl} - |F_{cal}|_{hkl} \right|}{\sum_{hkl} |F_{obs}|_{hkl}} \qquad \ldots\ldots\ldots\ldots\ldots\ldots (33)$$

or
$$R_w = \left(\frac{\sum_{hkl} W_{hkl} (|F_o|_{hkl} - |F_c|_{hkl})^2}{\sum W_{hkl} |F_o|_{hkl}^2} \right)^{-1/2} \quad \ldots\ldots\ldots\ldots\ldots\ldots\ldots\ldots (34)$$

The " Goodness of fit " index, is defined by :

$$\left(\frac{\sum_{hkl} W_{hkl} (|F_o|_{hkl} - |F_c|_{hkl})^2}{(n-m)} \right)^{1/2} \quad \ldots\ldots\ldots\ldots\ldots\ldots\ldots\ldots (35)$$

where n and m are numbers of observation and variables, respectively.

(9) : FOURIER SYNTHESIS (50-53)

It is possible to calculate ρ (x,y,z) using equation(17) when the approximate positions of the atoms and thermal parameters are known. Thus, by using the refined co-ordinates and temperature factors of a heavy atom found from a Patterson synthesis, a set of approximately correct phases may be calculated. The Fourier synthesis calculated using the observed values of $|F_{hkl}|$ and the calculated phases usually shows the positions of further atoms in the structure as electron density maxima. The parameters for the newly found atoms can be refined by the least-squares method and a new, better set of phases obtained, which in turn, will produce an improved Fourier synthesis. The process is repeated until all the atoms are found.

It is possible to calculate a Fourier synthesis using the differences between the 'observed' and 'calculated' structure factors. In such a synthesis, the contributions of the atoms which were used to calculate F_c are 'subtracted' out and the remaining features of the structure are shown more clearly.

(10) : THE DIRECT METHOD FOR SOLVING THE PHASE PROBLEM[54-56]

The method for solving the phase problem by using the Patterson function has been discussed. For most centrosymmetric space groups, in which the phase problem means simply finding a plus or minus sign for each observed structure amplitude, the Direct method can also be used conveniently.

In this method, all structure amplitudes $|F_{obs}|$, after corrections been made, are converted to the normalized structure factors E[57], where

$$E_{hkl}^2 = \frac{F_{hkl}^2}{\epsilon} \cdot \frac{1}{\sum_{\substack{j \text{ atoms} \\ \text{in cell}}} f_j^2} \quad \ldots\ldots(36)$$

N is the total number of atoms in the atoms in the cell and f_j is the atomic scattering factor. ϵ is an integer which is used to adjust the data at a symmetrical location in reciprocal space, for example, in space group $P2_1/c$, $\epsilon = 2$ for h 0 l and 0 k 0 reflections and $\epsilon = 1$ for the rest. Then the E values are scaled such that the average $E^2 = 1$.

The basis of this method is described by Sayre[58] in 1952. It can be shown that :

$$F_{hkl} = \phi_{hkl} \sum_{h'} \sum_{k'} \sum_{l'} F_{h'k'l'} \cdot F_{h-h',k-k',l-l'} \quad \ldots\ldots(37)$$

where ϕ_{hkl} is a calculable scaling term. The equation means that any structure factor F_{hkl} is determined by the product of all the pairs of structure factors, whose indices add to give (h,k,l). Sayre pointed out that for the case where F_{hkl} is large, the series must tend strongly in one direction (+ or -) and this direction is generally determined by the agreement in sign among products between large F's. Thus for three large reflections,

$$S (F_{hkl}) \sim S (F_{h'k'l'}) . S(F_{h-h',k-k',l-l'}) \quad \ldots\ldots\ldots(38)$$

Practically, only those reflections whose normalized structure factors are greater than a certain value E_{max} (e.g. 1.5) are used. All groups of reflections related by : h,k,l; h',k',l'; h-h',k-k',l-l' are sorted out. Up to three reflections are chosen to fix the origin and given positive signs. None may be (even,even, even), the parity of the second must differ from the first, and the parity of the third must differ from both the others and their sum.

M more reflections (M can be up to six) are chosen which should not all have even, even, even parity. These, together with the origin determing reflections, form the starting set. Signs are given to the E_{hkl} values of each of the M reflections,

and since they can either be positive or negative, there are 2^M possible combinations. The starting set are then used 2^M times in the following equation :

$$S\left(E_{hkl}\right) \sim S\left[\sum_{h'k'l'} \sum\sum\sum E_{h'k'l'} \cdot E_{h-h'\ k-k'\ l-l'}\right] \quad \ldots\ldots\ldots\ldots(39)$$

where S means 'sign of ' and $\sim$ means'probably equal to'.

The reflections are selected from the list of reflections starting with the lowest rank (most intense) and working up.

By expanding the set of phases, which are either retained or discarded depending on their agreement with those previously determined, more terms are entered into the summation, and the requirement for higher intensity reflections lessened. The starting set, within any one of the 2^M tries, are not allowed to change sign.

After the treatment of NR reflections 2^M times, the phasing information is summarized and compared, i.e., the number of cycles used for a run, the numbers of positive and negative reflections in the set and consistency index C which defined as :

$$C = \frac{\left\langle \left| E_{hkl} \cdot \sum\sum\sum E_{h'k'l'} \cdot E_{h-h'\ k-k'\ l-l'} \right| \right\rangle}{\left\langle |E_{hkl}| \cdot \sum\sum\sum |E_{h'k'l'}| \cdot |E_{h-h'\ k-k'\ l-l'}| \right\rangle} \quad \ldots\ldots\ldots\ldots(40)$$

where $\langle \quad \rangle$ means averaged over all h,k,l.

The correct solution should have :

(a) Highest consistency.

(b) Approximate equal numbers of '+' and '-'.

(c) Number of cycles should be least.

The reduced set of phases are used in computing a Fourier synthesis, which, if the correct solution has been chosen, will show some or all of the structure. Thereafter a series of least-squares cycles and Fourier calculations are used to complete the structure solution.

SECTION III EXPERIMENTAL

PART (A) INTRODUCTION

Three compounds (1) : π-$C_5H_5Fe(CO)PPh_3CF(CF_3)_2$, (2) : π-$C_5H_5Fe(CO)(PPh_3)CF_2CF_3$ and (3) : π-$C_5H_5Co(I)(PPh_3)CF_2CF_3$ were supplied by professor M.C.Baird of Queen's university, Kingston, Ontario. All three compounds are resonably soluble in CH_2Cl_2, benzene, and acetone, but are much less soluble in ethanol, ethyl ether and saturated hydrocarbons. They are all somewhat air-sensitive in solution.

Recrystallization of the three compounds was done in this laboratory. Fluorfe 1 and Fluorfe 2 were recrystallized from a mixture of dichloromethane and hexane. Since CH_2Cl_2 is very volatile, it evaporates more rapidly, leaving the compounds in hexane in which they are rather insoluble. Well shaped red and yellow crystals were obtained from Fluorfe 1 and Fluorfe 2 respectively. Fluorfe 3 was recrystallized from methanol and dark brown crystals obtained.

PART (B) INSTRUMENTAL TECHNIQUE

A single crystal of the right size, which appeared to be whole under a microscope, was selected. It was afixed to a borosilicate glass fibre using a mixture of glyptal cement and amyl acetate. The fibre was in turn fixed securely to a flexible copper wire attached to a goniometer head. The head was mounted on the goniometer in such a way that the crystal would be bathed in the diffractometer x-ray's beam.

The Weissenberg and oscillation photographs of the three crystals under investigation were obtained on a Charles Supper Co. Precession Camera.

A molybdenum fine focus x-ray tube was powered at 40 KV and 20 mA by a Picker Nuclear x-ray generator (model number 809 B). The wavelength of the molybdenum radiation filtered with Zirconium foil was taken as 0.71069 Å. The films used were Kodak 'No screen'.

The data was collected by a Picker Nuclear automated four- circle diffractometer operated by a P.D.P 8/s dedicated mini-computer. A Picker Nuclear constant potential diffraction generator (model number 6238 E - stable to within 0.1 KV and 0.02 mA) provided the power (40 KV 18 mA) for a molybdenum x-ray tube. The take off angle was 3.0° for the direct beam and

this was monochromated using the (0 0 2) face of a graphite monochromator 'crystal '.

The 0.71069 A K_α radiation of molybdenum was passed through a 1 mm. diameter pinhole collimator directed at the sample crystal. The sample was situated 14.0 cm from the point at which the x-rays were monochromated. Diffraction at the crystal took place in a plane perpendicular to that of monochromation. A receiving aperture whose size was determined by horizontal and vertical slits was located 23.0 cm from the crystal and 2 cm from a scintillation counter.

The detector was operated at about 1000 volts (5.60 helipot setting) and the pulse height analyser was set to receive 100% of the x-rays MoK_α intensity. A scan, using a 0.2 KeV window (upper level setting of 2.0 and 10% mode), of peak intensity versus baseline discriminator level was recorded from 10.0 KeV to 0.6 KeV. The differential pulse height distribution curve so obtained was used to establish the upper and lower level of discriminator voltage for 100% peak acceptance.

The centering of reflections was done by a P.D.P 8/s computer alignment program supplied by the Picker Nuclear Co.

For this process, the slits in the receiving collimator were partly shut to ensure higher accuracy. Counting at each angular setting was for 10 second periods. Location of half intensity on both sides of the peak permitted the computation of the peak center. Accurate values of $2\theta, \omega, \chi$ and ϕ were obtained at both $+2\theta$ and -2θ (for the h k l and -h -k -l reflections) and the results were averaged.

A series of three nickel foil attenuators on a rotating disc were located at the aperture. Above 10^4 cps, attenuators made of nickel foil and calibrated to factors of 2.781, 7.959, and 38.190 were automatically inserted in the aperture for the most intense reflections. To ensure the crystal was not deteriorating or changing its position in relation to the orientation matrix during the collection of data, check reflections (usually axial) were monitored. Most often these reflections varied slightly in harmony and one was chosen to scale the data.

In determining these crystal structures, all computing was done on the Control Data Corporation (C.D.C) Cyber 70 computer. Computer programs used are as follows :
Program PREP was used for data reduction. It brought all the counts to common basis by applying the attenuator factors to peak counts and backgrounds. The intensity of the strongest

selected check reflection was used to scale the data to a common standard for all reflections. The mean atomic scattering factors, at intervals of $\sin\theta/\lambda$ of 0.05 Å^{-1}, for all atoms were obtained from the computation of Ibers and others.[68] This program interpolated the scattering factor f_j for an atom j depending on the particular $\sin\theta/\lambda$ value of the reflection concerned.

Program NORMA prepared normalized structure factors for input to REL. It scaled the E values such that the average $E^2 = 1$. It also print out the numbers of E_{hkl} which were greater than 1.0, 2.0, and 3.0 respectively.

Program REL used the output data of NORMA to compute the phase for each reflections by the Direct method. Several parameters were involved in this program and are explained as follows :

NBACK is a parameter used to determine how the signs are treated. If NBACK is set equal to 0, as soon as a new sign is determined in the first cycle, the reflections whose signs had not been determined earlier are reexamined. In subsequent cycles, the moment a new sign is determined, it used to determine new signs further down the list only. Recycling continues until there are no more changes, or to a preset maximum number.

If NBACK is set equal to 1, the new signs determined are not used to determine further signs until the first of the cycles is finished.

P is the probability of the event that a sign has been correctly determined. This probability depends upon the mannitude of the normalized structure factors as well as the value PROBK which is approximately equal to $N^{-1/2}$ (where N is the number of atoms in the unit cell).

PROB1 is a minimum value for P below which the newly determined sign will not be used in further phasing.

PROB2 is the minimum value of P for a phase to be considered determined in the output

$$P = 0.5 + 0.5 \tanh \left[1/\sqrt{N \left(E_{hkl} \; E_{h'k'} + E_{h-h' \; k-k' \; \ell-\ell'} \right)} \right] \qquad \ldots\ldots\ldots\ldots\ldots\ldots (41)$$

Program RELFOR was used to process the solutions and pass a chosen solution to FORDAP.

Program FORDAP was used to calculate the Patterson function, Fourier, and difference Fourier syntheses.

Program SFLS was used for structure factor calculations and Least Squares refinement.

Program NUCLS$_4$ refined certain parts of the molecules as if they were regid bodies. For calculating structure factors, the rigid group contributions were summed separately from non-rigid atomic contributions. The Least squares process was similar to that in

SFLS except that separation of the problem into small matrices was not possible.

Program UTILITY was used to compute the geometry for the molecule whose atomic positions had been determined. Also it analysed thermal parameters in terms of ellipsoids. The program first converted the positional fractional coordinates to orthogonalized coordinates and the bond lengths angles etc., were computed using standard techniques. The standard deviation of a bond length, σ_l was computed using the following equation :

$$\sigma_l = \sqrt{(\sigma^2_{x1} + \sigma^2_{x2})\left(\frac{\Delta x}{l}\right)^2 + (\sigma^2_{y1} + \sigma^2_{y2})\left(\frac{\Delta y}{l}\right)^2 + (\sigma^2_{z1} + \sigma^2_{z2})\left(\frac{\Delta z}{l}\right)^2} \quad \ldots\ldots\ldots(42)$$

where σ_{x1} and σ_{x2} are the estimated standard deviation in the x parameter of atoms 1 and 2 respectively and l is the bond length.

Program DRAFT was used to draw the molecules in a 'ball and stick' form. It also drew the packing diagrams showing how the molecules pack in the unit cell.

PART (C) STRUCTURE DETERMINATIONS

(1) : THE MOLECULAR AND CRYSTAL STRUCTURE OF π-$C_5H_5Fe(CO)(PPh_3)CF(CF_3)_2$

Interpretion of Weissenberg h 0 ℓ, h 1 ℓ and precession h k 0, h k 1, 0 k 1, 1 k ℓ levels gave the following information : the Laue symmetry 2/m indicated a monoclinic space group; h 1 ℓ has twice the number of spots on h 0 ℓ; on h 0 ℓ, ℓ = 2n were present, ℓ = 2n+1 were absent. On h 1 ℓ, all ℓ were present. This implies a c glide perpendicular to b. From the precession photographs, along 0 k 0, k=2n was present and k=2n + 1 was absent. This implied a 2 fold screw axis existing parallel to b. Thus the space group was $P2_1/c$ (No.14).

The unit cell parameters were determined as follows :

a	9.219 (8) Å	V	2426.09 Å^3
b	9.135 (4) Å	M.W.	579.83 amu
c	28.834 (17) Å	Z	4
α	90.00°	d_{cal}	1.588 g cm^{-1}
β	92.43° (2)		
γ	90.00°		

There were 2421 reflections collected in the hemisphere ± h k ℓ to $2\theta_{max}$ = 45°. Only 1672 reflections for which I greater than 3σ(I) were used in the solution. Inspection of the sharpened three dimensional Patterson synthesis suggested 2 possible positions for the heavy atom iron, but only one position consistent with all Fe-Fe vectors. This

was at x = 0.025, y = 0.075, z = 0.125. This atom was used in calculation of the first approximate electron density synthesis $\rho(x\ y\ z)$ which was not very informative : The R factor at this point was 57.3%. The set of data were then treated by direct methods to obtain the phases. All reflections whose normalized structure factor E was greater than 1.5 were used. REL yielded a solution with 97.7% consistency using the following starting set :

h	k	ℓ	E
- 4	4	3	2.89
1	1	21	2.63
1	6	12	2.59
- 4	2	11	2.59
- 3	2	11	2.57
- 3	1	1	2.56
- 3	1	13	- 2.51

Fe, P, two phenyl rings and six fluorineswere shown by REL. The positions of the remaining atoms were yielded in the subsequent approximate electron density syntheses.

The structure was refined by the method of least squares using the full matrix method. The discrepancy index R at this stage dropped to 13.6 %. After five cycles of anisotropic temperature factor refinement, R was reduced to 6.8 % and R_w = 15.1 %. The 'Goodness of fit' index was 2.476.

Owing to computer memory restrictions, least squares refinement of positional and anisotropic thermal parameters necessitated dividing the parameters into three matrices. The final atomic parameters are given in TABLE (2).

RESULTS :

The geometric configuration of the molecule of π-$C_5H_5Fe(CO)(PPh_3)C_3F_7$ is shown in FIG.(13). TABLES(3) and (4) list bond length and bond angles, respectively. The averaged bond lengths and angles for the three phenyl rings and the cyclopentadiene ring are collected together in TABLE (5). The packing diagram is given in FIG.(14).

TABLE (2)

POSITIONAL AND ANISOTROPIC THERMAL PARAMETERS FOR Fluorfe 1*

		X	Y	Z
1	Fe	-0.09319(15)	-0.42756(16)	0.12803(5)
2	P	0.14723(26)	-0.42156(31)	0.11728(9)
3	O	-0.1711(8)	-0.4405(10)	0.0293(3)
4	F_{11}	-0.3614(5)	-0.1993(7)	0.1194(2)
5	F_{12}	-0.2206(6)	-0.1402(6)	0.0649(2)
6	F_{13}	-0.2574(7)	0.0099(6)	0.1203(2)
7	F_{31}	0.0047(6)	-0.2084(6)	0.2137(2)
8	F_{32}	-0.0732(7)	-0.0003(6)	0.1907(2)
9	F_{33}	-0.2239(6)	-0.1688(7)	0.2080(2)
10	F_{21}	0.0141(5)	-0.1278(5)	0.1182(2)
11	CP1	-0.1529(14)	0.3438(12)	0.1325(4)
12	CP2	-0.0596(13)	0.3849(12)	0.1725(4)
13	CP3	-0.1292(14)	0.4994(14)	0.1976(4)
14	CP4	-0.2681(13)	0.5329(13)	0.1728(4)
15	CP5	-0.2775(13)	0.4389(15)	0.1342(4)
16	C_1	-0.2392(11)	-0.1316(11)	0.1105(4)
17	C_2	-0.1038(10)	-0.2039(10)	0.1372(3)
18	C_3	-0.0997(10)	-0.1439(12)	0.1870(4)
19	C_4	-0.1350(10)	-0.4257(12)	0.0680(4)
20	C11	0.2192(10)	-0.3327(10)	0.0656(3)
21	C12	0.3073(10)	-0.3685(12)	0.0977(3)
22	C13	0.4275(11)	-0.2980(12)	0.0978(4)
23	C14	0.3409(11)	-0.2063(11)	-0.0123(3)
24	C15	0.1929(10)	-0.1808(11)	-0.0028(3)
25	C16	0.1323(10)	-0.2446(9)	0.0362(3)
26	C21	0.2207(10)	0.3946(10)	0.1082(3)
27	C22	0.1552(11)	0.3133(10)	0.0714(3)
28	C23	0.2116(13)	0.1764(12)	0.0602(4)
29	C24	0.3366(15)	0.1186(12)	0.0851(5)
30	C25	0.4010(12)	0.1997(13)	0.1211(4)
31	C26	0.3463(11)	0.3389(13)	0.1341(4)
32	C31	0.2566(9)	-0.3442(11)	0.1660(3)
33	C32	0.2634(10)	-0.4172(12)	0.1660(3)
34	C33	0.3405(11)	-0.3489(13)	0.2477(3)
35	C34	0.4087(11)	-0.2105(13)	0.2419(4)
36	C35	0.3974(12)	-0.1413(13)	0.1979(4)
37	C36	0.3230(10)	-0.2066(11)	0.1605(3)

* : Esd's are shown in parentheses. These are right justified to the least significant digit in the preceding number.

TABLE (2) cont.

		β_{11}*	β_{22}*	β_{33}*	β_{12}*	β_{13}*	β_{23}*
1	Fe	72.7	78.5(22)	7(2)	-12.6(22)	-0.3(5)	1.9(7)
2	P	70.9(39)	69.2(42)	8.4(4)	2.4(38)	-1.2(10)	1.6(13)
3	O	199(14)	176(14)	8(1)	-33(12)	-13(3)	-4(4)
4	F_{11}	77(9)	215(12)	19(1)	-13(8)	-6(2)	9(3)
5	F_{12}	164(10)	162(10)	11(17)	48(8)	-2(2)	10(3)
6	F_{13}	189(11)	102(10)	23(1)	73(8)	-12(3)	-11(3)
7	F_{31}	165(10)	153(11)	11(1)	21(8)	-17(2)	-14(2)
8	F_{32}	198(11)	111(10)	19(1)	-2(9)	-5(3)	-20(3)
9	F_{33}	144(10)	216(12)	13(10)	25(9)	11(2)	-16(3)
10	F21	90(8)	79(8)	14(1)	-12(7)	8(2)	-2(2)
11	CP1	165(22)	72(18)	17(2)	-88(18)	0(6)	15(5)
12	CP2	166(21)	98(20)	12(2)	-39(17)	7(6)	24(5)
13	CP3	124(21)	128(20)	14(2)	-14(17)	13(6)	21(6)
14	CP4	136(20)	133(24)	13(2)	-24(17)	21(5)	17(6)
15	CP5	134(21)	108(20)	17(2)	-34(18)	4(6)	21(6)
16	C_1	146(19)	107(19)	10(2)	17(15)	2(3)	-3(5)
17	C_2	104(14)	83(16)	6(1)	20(13)	2(4)	-2(4)
18	C_3	93(16)	130(19)	14(2)	22(14)	4(4)	-1(5)
19	C_4	76(16)	74(16)	17(2)	-4(15)	15(5)	9(6)
20	C_{11}	91(16)	68(16)	7(2)	-22(13)	6(4)	-6(4)
21	C_{12}	94(16)	148(20)	8(2)	-29(14)	9(4)	-1(5)
22	C_{13}	123(17)	138(19)	10(2)	-4(15)	3(4)	4(5)
23	C_{14}	157(19)	94(17)	9(2)	-49(15)	-3(4)	-4(5)
24	C_{15}	101(16)	96(17)	10(2)	-23(14)	-1(4)	0(5)
25	C_{16}	125(16)	42(14)	4(1)	-17(13)	-8(4)	4(4)
26	C_{21}	61(14)	69(17)	9(2)	23(13)	9(4)	3(4)
27	C_{22}	144(17)	81(17)	8(2)	-2(14)	9(4)	-14(4)
28	C_{23}	150(21)	104(20)	16(2)	0(17)	10(5)	-3(5)
29	C_{24}	184(23)	99(21)	15(2)	6(17)	22(6)	0(6)
30	C_{25}	129(18)	98(20)	19(2)	15(17)	8(5)	10(6)
31	C_{26}	89(17)	109(20)	16(2)	26(16)	9(5)	14(5)
32	C_{31}	43(14)	105(16)	9(2)	-18(13)	-3(4)	-12(5)
33	C_{32}	116(17)	131(18)	7(2)	14(16)	-6(4)	6(5)
34	C_{33}	76(16)	180(21)	10(2)	16(16)	-6(4)	-11(5)
35	C_{34}	75(16)	144(22)	17(2)	-31(16)	2(5)	-7(6)
36	C_{35}	137(20)	139(21)	11(2)	-17(16)	-3(5)	0(6)
37	C_{36}	76(15)	120(18)	10(2)	-29(14)	1(4)	-5(5)

*: of the form EXP [$-h^2\beta_{11}+k^2\beta_{22}+l^2\beta_{33}+2hk\beta_{12}+2hl\beta_{13}+2kl\beta_{23}$]

TABLE (3)

PRINCIPAL INTERMOLECULAR BOND DISTANCES(Å)*

Fe-P	2.252(3)	CP_1-CP_2	1.46(2)
Fe-C_2	2.063(9)	CP_2-CP_3	1.44(2)
Fe-C_4	1.76(1)	CP_3-CP_4	1.47(2)
C_4-O	1.16(1)	CP_4-CP_5	1.41(2)
P-C_{11}	1.846(9)	CP_5-CP_1	1.44(2)
P-C_{21}	1.834(9)	C_{11}-C_{12}	1.42(1)
P-C_{31}	1.836(10)	C_{12}-C_{13}	1.42(1)
C_2-F_{21}	1.42(1)	C_{13}-C_{14}	1.43(1)
C_2-C_1	1.58(1)	C_{14}-C_{15}	1.42(1)
C_1-F_{11}	1.32(1)	C_{15}-C_{16}	1.40(1)
C_1-F_{12}	1.33(1)	C_{16}-C_{11}	1.40(1)
C_1-F_{13}	1.34(1)	C_{21}-C_{22}	1.41(1)
C_2-C_3	1.54(1)	C_{22}-C_{23}	1.40(1)
C_3-F_{31}	1.34(1)	C_{23}-C_{24}	1.43(2)
C_3-F_{32}	1.34(1)	C_{24}-C_{25}	1.39(2)
C_3-F_{33}	1.34(1)	C_{25}-C_{26}	1.42(2)
C_{31}-C_{32}	1.41(1)	C_{26}-C_{21}	1.44(1)
C_{32}-C_{33}	1.44(1)	Fe-CP_1	2.17(1)
C_{33}-C_{34}	1.42(2)	Fe-CP_2	2.15(1)
C_{34}-C_{35}	1.42(2)	Fe-CP_3	2.15(1)
C_{35}-C_{36}	1.39(2)	Fe-CP_4	2.14(1)
C_{36}-C_{31}	1.41(1)	Fe-CP_5	2.11(1)

* : The [illegible]'s shown in parenthesis.

TABLE (4)

PRINCIPAL BOND ANGLES* IN Fluorfe 1 (deg.)

$FePC_{11}$	120.8(3)	FeC_4O	171.7(10)
$C_{11}PC_{21}$	98.1(4)	C_4FeC_2	96.2(4)
$C_{11}PC_{31}$	104.2(4)	$PFeC_2$	92.6(3)
$FePC_{31}$	114.6(3)	C_4FeP	92.3(3)
$FePC_{21}$	111.7(3)	$PFeC_4$	92.3(3)
$C_{21}PC_{31}$	105.5(4)	C_4FeCp	115.1(5)
FeC_2C_1	113.0(6)	CpFeP	120.0(5)
FeC_2F_{21}	113.2(6)	C_2FeCp	125.8(2)
FeC_2C_3	118.3(7)		
$C_1C_2C_3$	107.1(8)		
$C_3C_2F_{21}$	101.4(7)		
$C_1C_2F_{21}$	102.0(7)		
$F_{21}C_2C_3$	101.4(7)		
$F_{21}C_2C_1$	102.0(7)		
$C_3C_2C_1$	107.1(8)		

* The esd's shown in parenthesis.

TABLE (5)

RING PARAMETERS FOR Fluorfe 1*

		PHENYL RING 1		PHENYL RING 2	
BOND DISTANCE (A)	C_{31}-C_{32}	1.41(1)	C_{11}-C_{12}	1.42(1)	
	C_{32}-C_{33}	1.44(1)	C_{12}-C_{13}	1.42(1)	
	C_{33}-C_{34}	1.42(2)	C_{13}-C_{14}	1.43(1)	
	C_{34}-C_{35}	1.42(2)	C_{14}-C_{15}	1.42(1)	
	C_{35}-C_{36}	1.39(2)	C_{15}-C_{16}	1.40(1)	
	C_{36}-C_{31}	1.41(1)	C_{16}-C_{11}	1.40(1)	
	AVERAGES	1.42(2)	AVERAGES	1.40(1)	
BOND ANGLE (deg.)	$C_{36}C_{31}C_{32}$	121.2(9)	$C_{12}C_{11}C_{16}$	122.4(8)	
	$C_{33}C_{32}C_{31}$	118.6(9)	$C_{11}C_{12}C_{13}$	118.2(9)	
	$C_{34}C_{33}C_{32}$	120.0(1)	$C_{12}C_{13}C_{14}$	120.1(9)	
	$C_{33}C_{34}C_{35}$	119.0(1)	$C_{13}C_{14}C_{15}$	119.7(9)	
	$C_{36}C_{35}C_{34}$	121.0(1)	$C_{16}C_{15}C_{14}$	120.3(9)	
	$C_{35}C_{36}C_{31}$	120.0(1)	$C_{11}C_{16}C_{15}$	119.2(8)	
	AVERAGES	120.1(9)	AVERAGES	119.9(9)	
PLANE DEVIATIONS	C_{31}	-0.002605	C11	-0.003687	
	C32	0.001030	C12	0.011194	
	C_{33}	0.001601	C13	-0.011439	
	C_{34}	-0.002694	C14	0.004134	
	C_{35}	0.001178	C15	0.003512	
	C_{36}	0.001489	C16	-0.003715	

TABLE (5) CONT.

		PHENYL RING 3		CYCLOPENTADIENYL RING	
BOND DISTANCE (A)	C_{21}-C_{22}	1.41(2)	Cp1-Cp2	1.46(2)
	C_{22}-C_{23}	1.40(2)	Cp2-Cp3	1.44(2)
	C_{23}-C_{24}	1.43(2)	Cp3-Cp4	1.47(2)
	C_{24}-C_{25}	1.39(1)	Cp4-Cp5	1.41(2)
	C_{25}-C_{26}	1.42(2)	Cp5-Cp1	1.44(2)
	C_{26}-C_{21}	1.44(2)	AVERAGES	1.44(2)
	AVERAGES	1.42(2)		
BOND ANGLE (deg.)	$C_{22}C_{21}C_{26}$	120.8(9)	Cp5Cp1Cp2	105.0(1)
	$C_{21}C_{22}C_{23}$	119.5(9)	Cp1Cp2Cp3	109.0(1)
	$C_{22}C_{23}C_{24}$	121.0(1)	Cp2Cp3Cp4	108.0(1)
	$C_{23}C_{24}C_{25}$	119.0(1)	Cp3Cp4Cp5	106.0(1)
	$C_{24}C_{25}C_{26}$	122.0(1)	Cp4Cp5Cp1	112.0(1)
	$C_{21}C_{26}C_{25}$	118.0(1)	AVERAGES	108.0(1)
	AVERAGES	120.1(9)		
PLANE DEVIATIONS	C_{21}	-0.001632	Cp1	0.006627
	C_{22}	-0.005544	Cp2	-0.005565
	C_{23}	0.005140	Cp3	0.002452
	C_{24}	-0.000704	Cp4	0.001840
	C_{25}	-0.003185	Cp5	-0.005354
	C_{26}	0.002661		

FIGURE (13)

THE CONFIGURATION OF THE π-$C_5H_5Fe(CO)(PPh_3)CF(CF_3)_2$ MOLECULE

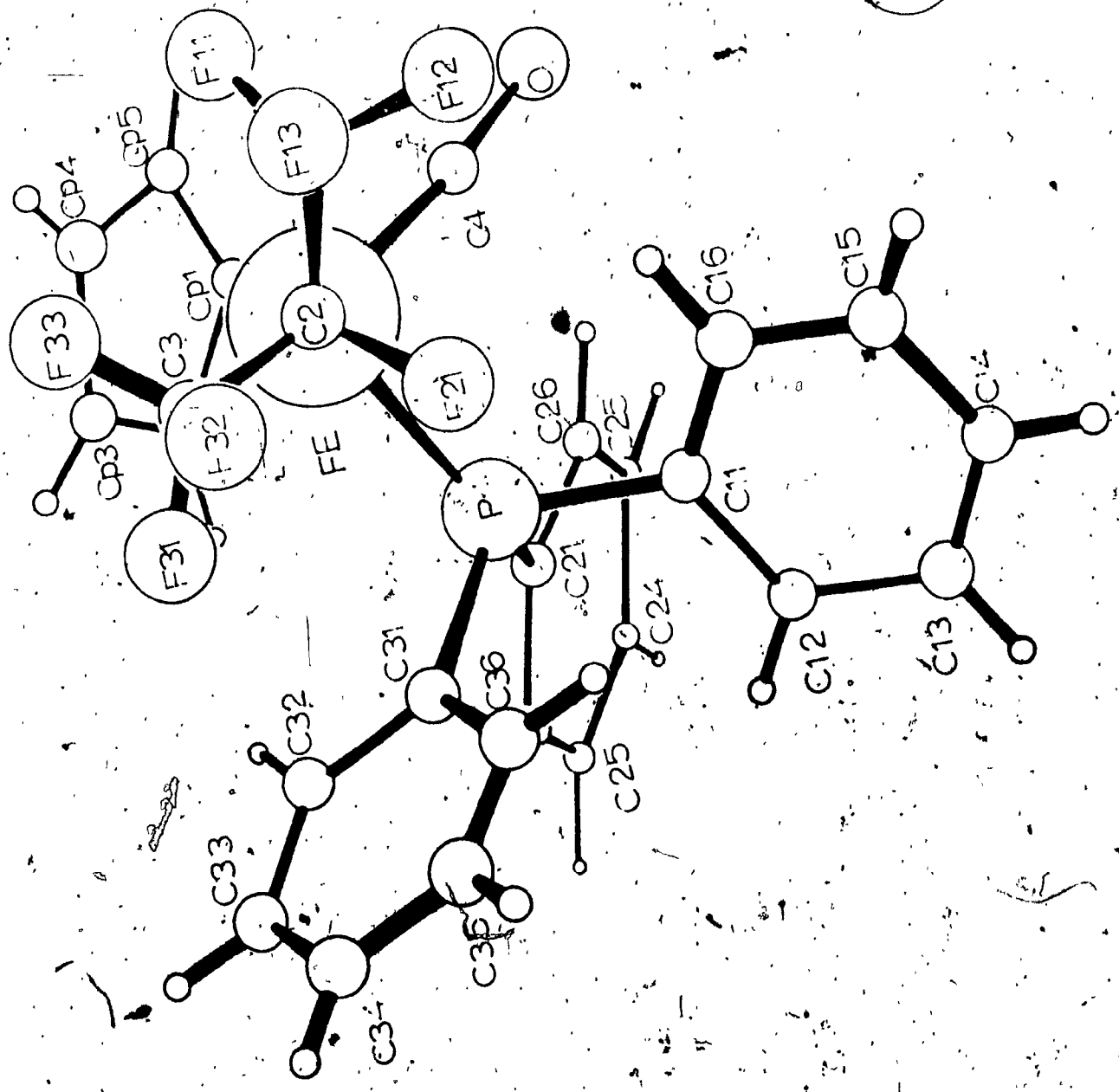
F11
F13
F12
O
C4
CP5
CP4
CP1
C2
C3
F33
F32
F31
CP3
FE
F21
P
C26
C25
C16
C15
C14
C11
C12
C13
C21
C24
C31
C36
C32
C25
C33
C35
C34

FIGURE (14)

THE PACKING DIAGRAM OF π-$C_5H_5Fe(CO)(PPh_3)CF(CF_3)_2$

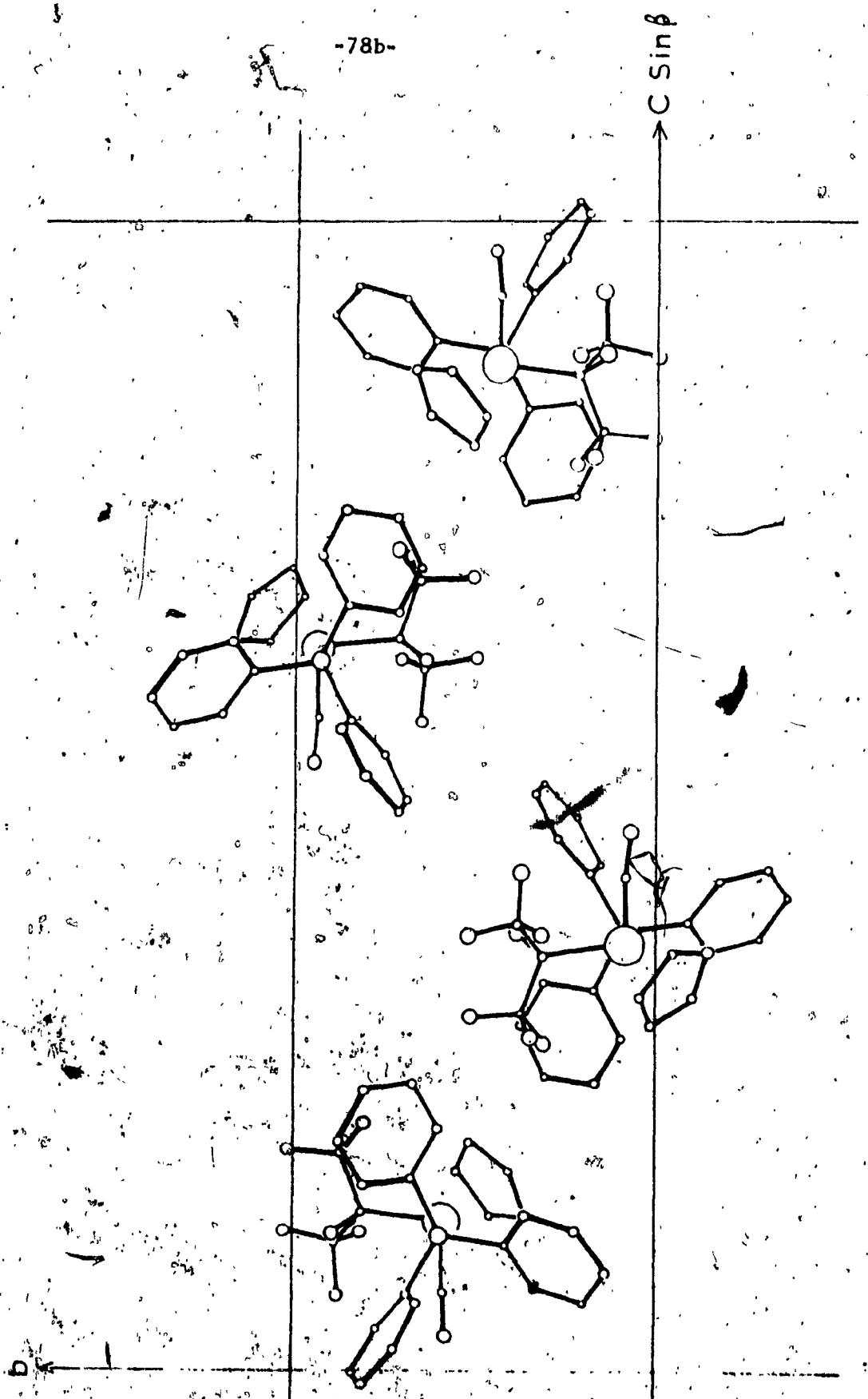
C Sinβ
b

(2) MOLECULAR AND CRYSTAL STRUCTURE OF π-$C_5H_5Fe(CO)(PPh_3)CF_2CF_3$

Interpretation of Weissenberg 0,k,ℓ; 1,k,ℓ; and precession h,k,0; h,k,1; h,0,k; h,0,ℓ photographs; limited the space group assignment to $P2_1/c$ (No.14) as describe before, but the Weissenberg rotation axis was "a" this time while in π-$C_5H_5Fe(CO)(PPh_3)CF(CF_3)_2$ it had been "b".

The unit cell parameters are listed as follows :

a	11.843(7) Å	V	2339.10 Å^3
b	10.510(24) Å	M.W.	529.83 amu
c	18.807(12) Å	Z	4
α	90.0°	d_{cal}	1.905 g cm^{-1}
β	87.75(2)°		
γ	90.00°		

The sharpened Patterson synthesis suggested the position for Fe at x=0.125, y=0.25, z=0.65. In view of the difficulties encountered with Fluorfe 1 , the data were treated by direct methods immediately : thus all reflections with normalized structure factors E greater than 1.5 were used to determine the phases initially, however, this did not work because too few reflections were used. After changing E_{min} to 1.3 and also PROB 1 and PROB 2 to 0.85, REL yielded a solution with 95% consistency using the following starting set :

h	k	ℓ	E
-6	1	0	3.12
1	1	0	2.67
-1	1	7	2.02
6	1	0	-3.03
-1	1	0	-2.65
1	2	4	2.48
-2	7	4	-2.41

A Fourier based on the output of REL showed two possible positions for P, one with y= 0.180 and another with y= 0.315. The former, having the larger peak, was used for a Fourier calculation. A Fourier based on Fe and P from REL showed more atoms : C_2, F_{21}, F_{22}, F_{33}, F_{32}, F_{31}. A structure factor calculation based on these atoms plus Fe and P was done : the R factor improved to 39% At this time, it was suspected the phosphorus position was not correct, so a fourier map was calculated based on Fe only, the R factor was 48.2%; it showed that the P position was at y= 0.315. This had been shown by REL before, but the wrong peak had been selected. This occured because the position of Fe at 0.240, yielded a pseudo mirror-plane at y= 0.250. The fourier based on Fe, P showed most of the structure (R factor 40.8%). The remaining atoms were all found after several cycles.

The reflection data of Fluorfe 2 were re-collected later and then averaged with the first set.

There a total of 5080 reflections collected in two sets of data but only 1427 above 3σ were used for the least squares. The first set of data was collected in the quarter sphere $\pm h, k, \ell$ with $2\theta_{max} = 45°$; the second set comprised the quarter sphere $h, k, \pm\ell$ with $2\theta_{max} = 30°$. The structure was refined by the method of full matrix least squares. Because the number of reflections was limited, the structure could only be refined isotropically. (Since anisotropic temperature factors have six parameter to refine, this requires considerably more observations.)

In an attempt to improve the overall quality of the structure, we refined the structure with rigid idealized phenyl rings (C-C = 1.39 Å). This reduced the 24 variables for one ring (18 positional variables plus six thermal parameters) to 12 variables for one rigid ring (X_c, Y_c, Z_c, θ, ρ, Φ) plus 6 thermal parameters. (X_c Y_c Z_c is the position of center of the ring; θ, ρ, Φ are orientation angles of the ring). Thus, a total of 72 parameters (including parameters for the rest of the molecule) were reduced to 36. The purpose in doing this was to try to let the remaining variables of the whole molecule refine better. Unfortunately, it did nothing to

improve the structure. The least squares isotropic refinement converged at R = 16.9% and R_w = 15.5% and the " Goodness of fit" is 3.976. The final atomic parameters are given in TABLE (6).

RESULTS :

The quality of this crystal structure is very unsatisfactory. The reason for this is that the reflection intensity was too weak due to the crystal being too small. It has not been possible to grow a larger crystal.

The geometric configuration of the molecule of FLUORFE 2 is shown in FIG.(15). The packing diagram is given in FIG.(16). TABLES (8) and (9) list the bond lengths and bond angles, respectively. The average bond lengths and angles for the cyclopendienyl ring are given in TABLE (10). Table (7) list the plane deviations for cyclopentadienyl ring.

TABLE (6) POSITIONAL AND ISOTROPIC THERMAL* PARAMETERS FOR Fluorfe 2**

		X	Y	Z	B (A^2)
1	Fe	-0.1273(4)	0.2404(6)	0.3527(3)	3.9(2)
2	P	-0.2878(9)	0.3113(9)	0.4018(6)	4.8(3)
3	O	-0.234(3)	-0.009(3)	0.321(2)	11(1)
4	C1	-0.190(4)	0.090(5)	0.331(3)	11(2)
5	C2	-0.124(11)	0.286(12)	0.245(6)	21(5)
6	F21	-0.136(3)	0.419(4)	0.245(2)	17(1)
7	F22	-0.261(2)	0.314(2)	0.241(1)	12(8)
8	C3	-0.097(12)	0.215(12)	0.163(8)	22(5)
9	F31	-0.115(2)	0.295(3)	0.132(1)	14(1)
10	F32	0.006(3)	0.209(3)	0.195(2)	13(1)
11	F33	-0.168(4)	0.134(5)	0.189(3)	17(2)
12	CP1	0.019(4)	0.298(6)	0.337(3)	15(2)
13	CP2	0.041(4)	0.178(5)	0.348(2)	6(1)
14	CP3	-0.007(4)	0.149(4)	0.424(2)	6(1)
15	CP4	-0.060(4)	0.276(5)	0.452(2)	8(1)
16	CP5	-0.009(4)	0.365(5)	0.392(3)	10(2)
17	RING1	-0.239(1)	0.606(2)	0.459(1)	
18	RING2	-0.3893(15)	0.1616(17)	0.5396(9)	
19	RING3	-0.5136(16)	0.3197(18)	0.3189(7)	

* : Isothermal parameters in A^2

** : Esd's are shown in parentheses. These are right justified to the least significant digit in the preceding number.

	PHI	THETA	RHO
RING 1	-0.59(4)	-1.19(2)	-0.41(4)
RING 2	-1.63(3)	-0.65(2)	3.99(2)
RING 3	0.51(3)	-0.08(2)	1.03(1)

TABLE (7) DEVIATIONS FROM THE PLANE FOR THE CYCLOPENTADIENYL RING

Cp1	-0.110525
Cp2	0.027165
Cp3	0.046290
Cp4	-0.093104
Cp5	0.130175

TABLE (8)

PRINCIPAL INTERMOLECULAR BOND DISTANCES(A)*

Fe-P	2.21(1)	C2-C3	1.7(2)
Fe-C2	2.07(12)	C3-F33	1.3(1)
Fe-C1	1.80(5)	C3-F31	1.1(1)
C1-O	1.18(6)	C3-F32	1.4(1)
P-C41	1.95(2)	CP1-CP2	1.31(8)
P-C51	1.84(3)	CP2-CP3	1.34(6)
P-C61	1.76(2)	CP3-CP4	1.55(7)
C2-F21	1.4(1)	CP5-CP4	1.56(7)
C2-F22	1.7(1)	CP5-CP1	1.29(8)

DISTANCES FROM IRON TO CYCLOPENTADIENE(A)*

Fe-CP1	1.85(5)
Fe-CP2	2.10(4)
Fe-CP3	2.21(4)
Fe-CP4	2.09(4)
Fe-CP5	2.08(5)
averaged	2.06(4)

* : The esd's shown in parenthesis.

TABLE (9)

PRINCIPAL BOND ANGLES* (deg)

$FePC_{51}$	117(1)	FeC_1O	176(4)
$FePC_{61}$	121(1)	C_1FeP	92(2)
$FePC_{41}$	106.0(9)	$PFeC_2$	108(4)
$C_{41}PC_{51}$	106(1)	C_1FeC_2	89(4)
$C_{41}PC_{61}$	108(2)	$F_{21}C_2F_{22}$	74(6)
$C_{51}PC_{51}$	99(1)	$F_{22}C_2C_3$	100(8)
FeC_2F_{21}	104(7)	$C_3C_2F_{21}$	116(9)
FeC_2F_{22}	96(6)	$PFeC_1$	93(2)
FeC_2C_3	140(8)	$C_1FeCp(av.)$	119.2(2)
$F_{22}C_2C_3$	100(8)	$CpFeP(av.)$	120(1)
$F_{21}C_2C_3$	116(9)		
$F_{21}C_2F_{22}$	74(6)		

*: The esd's shown in parenthesis.

TABLE (10)

BOND LENGTHS AND ANGLES FOR THE CYCLOPENDIENE RING

	ANGLES		BONDS
Cp5Cp1Cp2	106(4)	Cp1-Cp2	1.31(8)
Cp1Cp2Cp3	106(4)	Cp2-Cp3	1.54(6)
Cp2Cp3Cp4	98(3)	Cp3-Cp4	1.55(7)
Cp3Cp4Cp5	109(5)	Cp4-Cp5	1.56(7)
Cp4Cp5Cp1	116(5)	Cp5-Cp1	1.29(8)
averaged	107(4)		1.45(7)

FIGURE (15)

THE CONFIGURATION OF π-$C_5H_5Fe(CO)(PPh_3)CF_2CF_3$

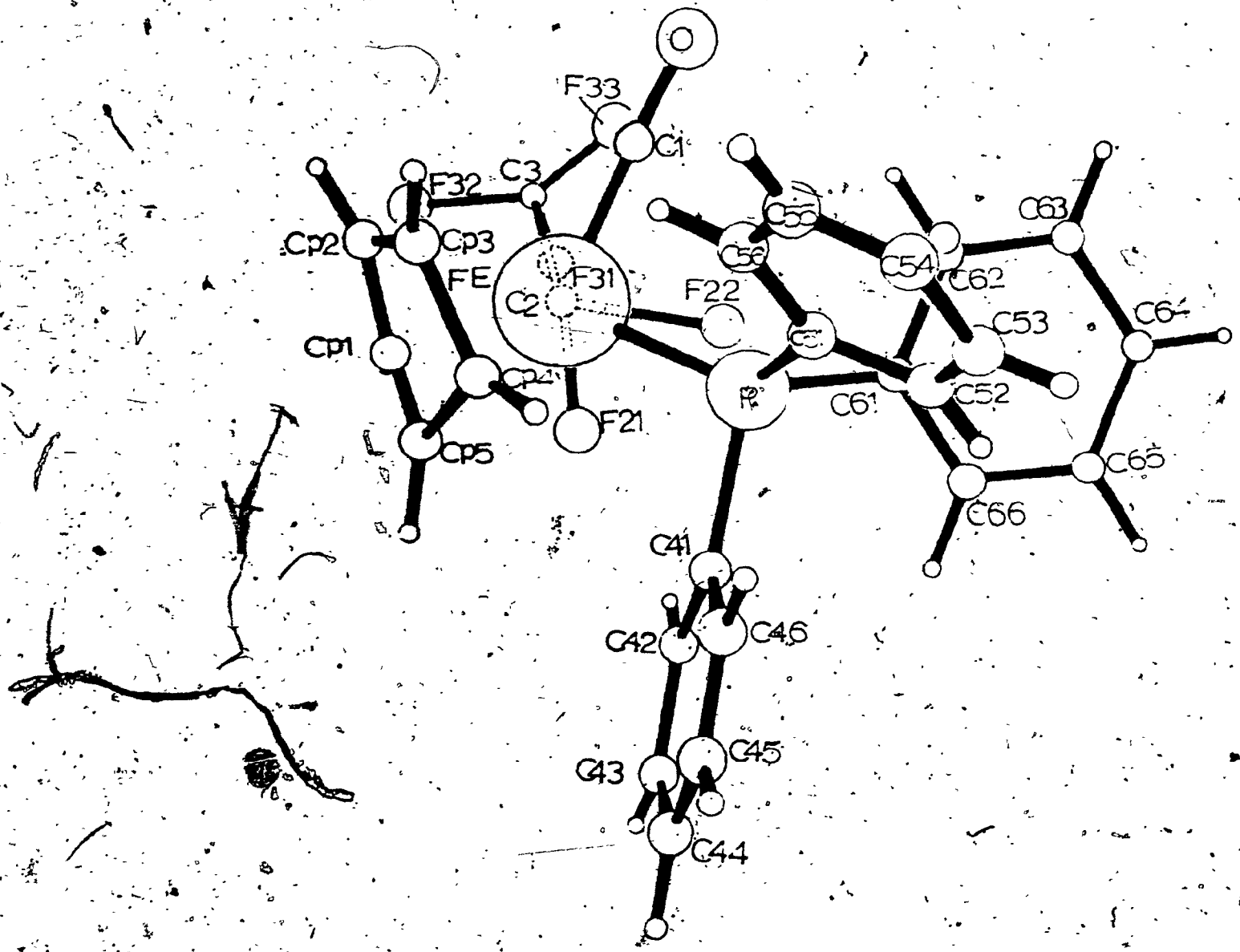
O
F33
C1
F32
C3
Cp2
Cp3
FE
C2
F31
F22
Cp1
Cp4
F21
Cp5
C56
C55
C54
C63
C62
C53
C64
C52
C61
C65
C66
C41
C42
C46
C45
C43
C44

FIGURE (16)

THE PACKING DIAGRAM OF π-$C_5H_5Fe(CO)(PPh_3)CF_2CF_3$

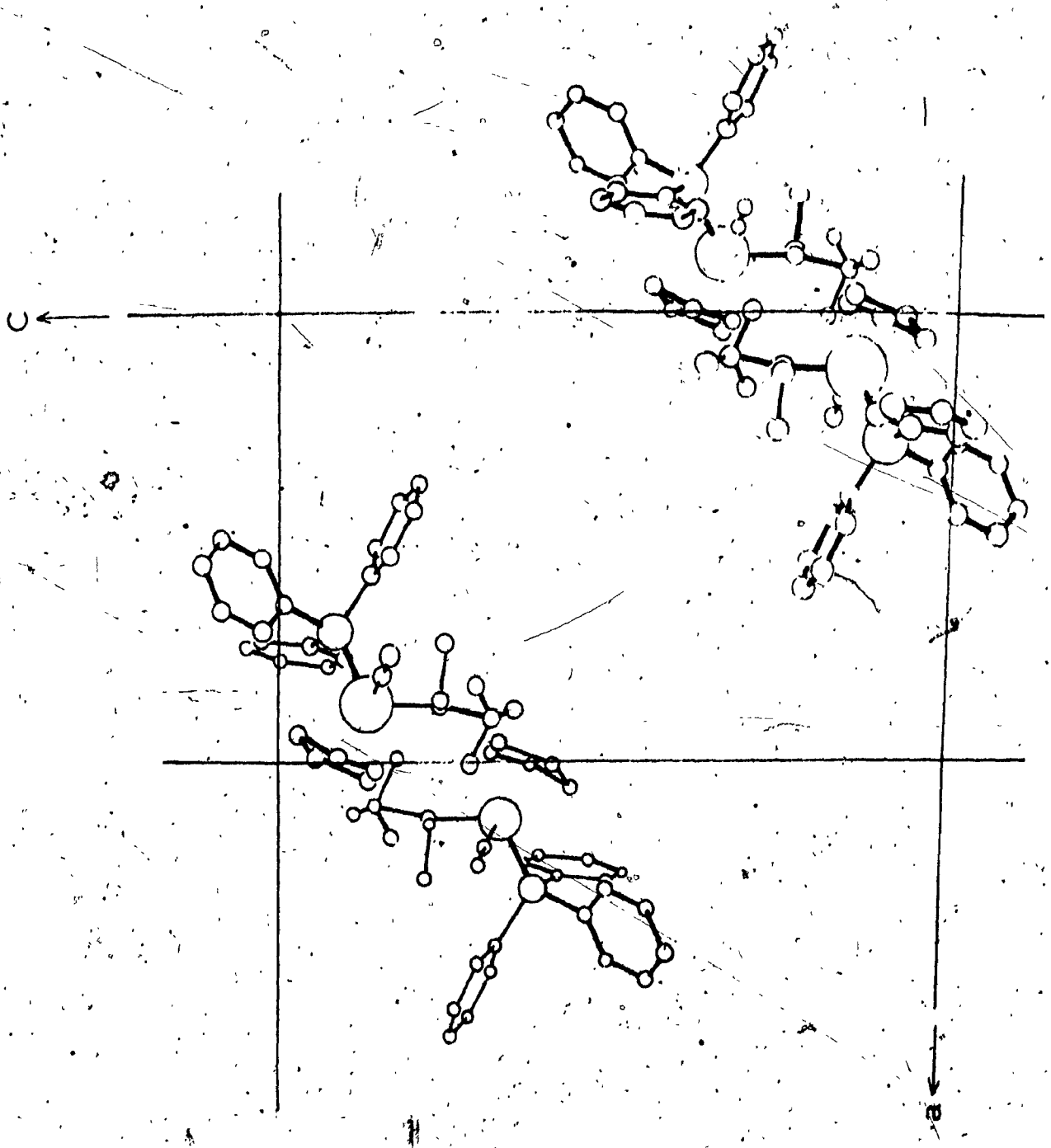
c
a

(3) THE MOLECULAR AND CRYSTAL STRUCTURE OF π-$C_5H_5Co(PPh_3)CF_2CF_3$

Interpretation of Weissenberg h,K,0;h,k,1 and precession h,0,ℓ; h,1,ℓ; 0,k,ℓ; 1,k,ℓ; photographs limited the space group assignment to P1 (No.1) or $P\bar{1}$ (No.2) of the triclinic crystal system. Thus there was no laue symmetry other than an inversion center. The crystal was mounted along the c axis.

The unit cell parameters are listed as follows:

a	9.564(4) Å	V	1222.46 Å^3
b	10.609(4) Å	M.W.	631.84 amu
c	12.058 (5) Å	d_{cal}	1.717 g cm^{-1}
α	91.50(2)	Z	2
β	92.32(2)		
γ	86.82(2)		

Reflections were collected in a hemisphere of $\pm h, \pm k, \ell$ with $2\theta_{max} = 45°$. A total of 3657 reflections were collected and 2458 reflections used in the least squares.

Inspection of the sharpened Patterson syntheses suggested the position for I at x = 0.16, y = 0.375, z = 0.175. The phase problem in this crystal was relatively easy solved since it contained I, a very heavy atom. This atom was used to run a structure factor calculation; the R factor was 43%. The position of the remaining atoms were found normally after several cycles.

The structure was refined by the method of least squares using a full matrix. The discrepancy index R reduced to 12.3% after isotropic refinement. The data were corrected for absorption at this point. The crystal dimensions were approximately 0.34 x 0.24 x 0.28 m.m. and the linear absorption coefficient was 21.29 cm^{-1}. Further refinements were done anisotropically, R converged to 5.9% and R_w converged to 5.4%. The 'Goodness of fit' was 2.333. The final atomic parameters are given in TABLE (11) and TABLE (12).

RESULTS :

The geometric configuration of the molecule of Fluorco is shown in FIG.(17). The packing diagram is given in FIG..(18). TABLES (13) and (14) list bond length and bond angles respectively. The averaged bond lengths and angles for the three phenyl rings and cyclopentadiene ring are collected together in TABLE (15).

TABLE (11) POSITIONAL PARAMETERS FOR Fluorco*

		X	Y	Z
1	I	0.13040(10)	0.48319(7)	0.21363(8)
2	Co	0.1927(2)	0.2573(1)	0.1367(1)
3	P	0.3023(3)	0.1898(2)	0.2985(2)
4	F_{11}	-0.240(1)	0.183(1)	0.134(1)
5	F12	-0.150(1)	0.360(1)	0.106(1)
6	F_{13}	-0.122(1)	0.203(1)	-0.007(1)
7	F_2	0.007(1)	0.064(1)	0.157(1)
8	F_3	-0.034(1)	0.216(1)	0.276(1)
9	CP1	0.316(1)	0.346(1)	0.020(1)
10	CP2	0.388(1)	0.229(1)	0.057(1)
11	CP3	0.296(1)	0.127(1)	0.030(1)
12	CP4	0.172(1)	0.174(1)	-0.025(1)
13	CP5	0.181(1)	0.310(1)	-0.032(1)
14	C11	0.207(1)	0.183(1)	0.429(1)
15	C12	0.149(1)	0.296(1)	0.474(1)
16	C13	0.080(2)	0.297(1)	0.575(1)
17	C14	0.069(1)	0.180(2)	0.632(1)
18	C15	0.124(2)	0.069(1)	0.587(1)
19	C16	0.193(1)	0.064(1)	0.483(1)
20	C21	0.377(1)	0.028(1)	0.274(1)
21	C22	0.523(1)	-0.001(1)	0.272(1)
22	C23	0.481(2)	-0.219(1)	0.221(1)
23	C24	0.333(1)	-0.192(1)	0.224(1)
24	C25	0.280(1)	-0.068(1)	0.250(1)
25	C26	0.577(1)	-0.123(1)	0.244(1)
26	C31	0.456(1)	0.279(1)	0.350(1)
27	C32	0.504(1)	0.381(1)	0.290(1)
28	C33	0.625(2)	0.436(1)	0.332(1)
29	C34	0.698(2)	0.398(1)	0.429(1)
30	C35	0.648(2)	0.299(1)	0.490(1)
31	C36	0.526(1)	0.242(1)	0.450(1)
32	C4	0.129(1)	0.238(1)	0.102(1)
33	C5	0.002(1)	0.192(1)	0.169(1)

* : Esd's are shown in parentheses. These are right justified to the least significant digit in the preceding number.

TABLE (12) ANISOTROPIC THERMAL PARAMETERS FOR Fluorco*(x 10^4)

		β_{11}	β_{22}	β_{33}	β_{12}	β_{13}	β_{23}
1	1	164.4(16)	72.4(8)	106.8(9)	-16.4(9)	-0.6(10)	4.8(6)
2	Co	85(3)	65(2)	57(1)	-19(2)	1(2)	8(1)
3	P	86(5)	64(3)	58(3)	-25(3)	0(3)	5(2)
4	F11	80(11)	267(13)	201(11)	-65(11)	-29(9)	68(10)
5	F12	171(15)	141(10)	263(14)	-7(10)	-55(11)	45(10)
6	F13	182(15)	379(19)	113(10)	-21(13)	-47(10)	-2(10)
7	F2	135(11)	107(7)	171(9)	-58(8)	-25(8)	31(7)
8	F3	111(10)	199(10)	81(6)	-55(8)	6(7)	18(6)
9	CP1	154(22)	159(17)	58(11)	-24(16)	44(13)	17(11)
10	CP2	132(22)	133(16)	78(12)	1(16)	50(13)	-15(11)
11	CP3	188(25)	123(15)	61(11)	-9(14)	21(13)	2(10)
12	CP4	164(22)	125(15)	55(10)	8(16)	-9(12)	-2(10)
13	CP5	167(24)	150(16)	43(10)	10(16)	24(13)	12(10)
14	C11	71(17)	130(14)	58(10)	-38(13)	-14(10)	-10(10)
15	C12	184(25)	152(17)	57(11)	15(17)	15(14)	-24(11)
16	C13	184(26)	207(20)	85(14)	24(19)	18(16)	-2(13)
17	C14	105(22)	241(24)	88(14)	-51(20)	7(14)	-17(15)
18	C15	180(27)	213(22)	69(13)	-94(21)	12(15)	24(14)
19	C16	140(21)	123(14)	87(12)	-59(14)	-14(13)	27(11)
20	C21	123(19)	66(11)	46(10)	2(13)	-9(11)	5(8)
21	C22	114(21)	102(14)	64(11)	1(14)	9(12)	3(9)
22	C23	248(30)	107(15)	72(12)	4(18)	20(16)	7(10)
23	C24	205(27)	82(13)	76(12)	-20(16)	-12(13)	6(10)
24	C25	213(25)	48(10)	84(12)	-52(14)	-12(14)	-4(9)
25	C26	181(25)	125(16)	100(13)	23(17)	13(15)	-12(11)
26	C31	110(18)	66(11)	69(10)	-47(12)	-5(11)	-12(8)
27	C32	105(19)	80(12)	146(14)	-55(13)	-4(14)	19(11)
28	C33	170(25)	128(16)	162(18)	-97(17)	-36(18)	24(14)
29	C34	195(27)	125(16)	124(15)	-84(17)	-54(17)	27(13)
30	C35	173(26)	150(18)	101(14)	-55(18)	-46(15)	-0(13)
31	C36	163(23)	134(15)	64(11)	-58(16)	-36(13)	3(10)
32	C4	121(24)	156(20)	112(16)	-48(18)	-30(16)	26(14)
33	C5	70(16)	985(11)	80(11)	-33(11)	1(11)	19(9)

* : of the form EXP $[-h^2\beta 11+k^2\beta 22+l^2\beta 33+2hk\beta 12+2hl\beta 13+2kl\beta 23]$.

TABLE (13)

PRINCIPAL INTERMOLECULAR BOND DISTANCES (Å)

Co-P	2.290(3)	C11-C12	1.40(2)
Co-I	2.595(1)	C12-C13	1.41(2)
Co-C_5	2.044(11)	C13-C14	1.45(2)
C_5-F_3	1.36(1)	C14-C15	1.37(2)
C_5-F_2	1.36(1)	C15-C16	1.44(2)
C_5-C_4	1.53(2)	C16-C11	1.45(2)
C_4-F_{13}	1.36(2)	C21-C22	1.42(2)
C_4-F_{11}	1.31(2)	C22-C26	1.41(2)
C_4-F_{12}	1.31(2)	C23-C26	1.42(2)
P-C_{11}	1.85(1)	C24-C23	1.43(2)
P-C_{21}	1.85(1)	C25-C24	1.41(2)
P-C_{31}	1.87(1)	C25-C21	1.42(2)
CP1-CP2	1.46(2)	C31-C32	1.43(1)
CP2-CP3	1.44(2)	C32-C33	1.40(2)
CP3-CP4	1.41(2)	C33-C34	1.39(2)
CP4-CP5	1.45(2)	C34-C35	1.41(2)
CP5-CP1	1.48(2)	C35-C36	1.40(2)
		C36-C31	1.41(2)

DISTANCES FROM COBALT TO CYCLOPENTADIENE(Å)

Co-C01	2.14(1)	Co-CP4	2.12(1)
Co-CP2	2.14(1)	Co-CP5	2.12(1)
Co-CP3	2.09(1)	Average : 2.12(1)	

TABLE (14)

PRINCIPAL BOND ANGLES*(deg)

$CoPC_{11}$	121.7(4)	$ICoC_5$	93.9(3)
$C_{11}PC_{21}$	105.3(5)	$PCoC_5$	95.4(3)
$C_{11}PC_{31}$	99.9(5)	ICoP	94.47(9)
$CoPC_{31}$	116.4(3)	$F_2C_5F_3$	105.4(8)
$CoPC_{21}$	108.0(3)	$F_3C_5C_4$	103.0(9)
$C_{21}PC_{31}$	103.8(5)	$C_4C_5F_2$	104.9(9)
CoC_5F_3	112.7(7)	PCoI	94.47(9)
CoC_5F_2	109.6(7)	ICoP(av.)	116.7(3)
CoC_5C_4	120.2(8)	CPCoP(av.)	118.4(3)
$C_4C_5F_3$	102.9(9)		
$C_4C_5F_2$	104.9(9)		
$F_2C_5F_3$	105.4(8)		

* : Esd's in parenthesis.

TABLE (15)

RING PARAMETERS FOR Fluorco*

		PHENYL RING 1		PHENYL RING 2	
BOND DISTANCE (A)	C_{11}-C_{12}	1.40(2)	C_{21}-C_{22}	1.42(2)
	C_{12}-C_{13}	1.41(2)	C_{22}-C_{26}	1.41(2)
	C_{13}-C_{14}	1.45(2)	C_{23}-C_{26}	1.42(2)
	C_{14}-C_{15}	1.37(2)	C_{24}-C_{23}	1.43(2)
	C_{15}-C_{16}	1.44(2)	C_{25}-C_{24}	1.41(2)
	C_{16}-C_{11}	1.45(2)	C_{25}-C_{21}	1.42(2)
	AVERAGES	1.42(2)	AVERAGES	1.42(2)
BOND ANGLE (deg.)	$C_{12}C_{11}C_{16}$	117.0(1)	$C_{25}C_{21}C_{22}$	121.0(1)
	$C_{11}C_{12}C_{13}$	121.0(1)	$C_{21}C_{22}C_{26}$	121.0(1)
	$C_{12}C_{13}C_{14}$	120.0(1)	$C_{22}C_{26}C_{23}$	118.0(1)
	$C_{13}C_{14}C_{15}$	120.0(1)	$C_{26}C_{23}C_{24}$	121.0(1)
	$C_{14}C_{15}C_{16}$	120.0(1)	$C_{23}C_{24}C_{25}$	120.0(1)
	$C_{15}C_{16}C_{11}$	122.0(1)	$C_{24}C_{25}C_{21}$	119.0(1)
	AVERAGES	120.0(1)	AVERAGES	120.0(1)
PLANE DEVIATIONS	C_{11}	0.013864	C_{21}	-0.004135
	C_{12}	-0.006577	C_{22}	0.008004
	C_{13}	-0.002405	C_{23}	-0.001279
	C_{14}	0.003668	C_{24}	0.005106
	C_{15}	0.003712	C_{25}	-0.002451
	C_{16}	-0.012263	C_{26}	-0.005245

TABLE (15) CONT.

	PHENYL RING 3		CYCLOPENTADIENYL RING	
BOND DISTANCE (A)	C_{31}-C_{32}	1.43(1)	Cp1-Cp2	1.46(2)
	C_{32}-C_{33}	1.40(2)	Cp2-Cp3	1.44(2)
	C_{33}-C_{34}	1.38(2)	Cp3-Cp4	1.41(2)
	C_{34}-C_{35}	1.41(2)	Cp4-Cp5	1.45(2)
	C_{35}-C_{36}	1.40(2)	Cp5-Cp1	1.48(2)
	C_{36}-C_{31}	1.41(2)	AVERAGES	1.45(2)
	AVERAGES	1.41(2)		
BOND ANGLE (deg.)	$C_{36}C_{31}C_{32}$	120.0(1)	Cp5Cp1Cp2	106.0(1)
	$C_{31}C_{32}C_{33}$	117.0(1)	Cp1Cp2Cp3	108.0(1)
	$C_{32}C_{33}C_{34}$	124.0(1)	Cp2Cp3Cp4	110.0(1)
	$C_{33}C_{34}C_{35}$	119.0(1)	Cp3Cp4Cp5	107.0(1)
	$C_{34}C_{35}C_{36}$	118.0(1)	Cp4Cp5Cp1	109.0(1)
	$C_{35}C_{36}C_{31}$	121.0(1)	AVERAGES	108.0(1)
	AVERAGES	120.0(1)		
PLANE DEVIATIONS	C_{31}	-0.019504	Cp1	0.006807
	C_{32}	0.008727	Cp2	-0.008775
	C_{33}	0.005668	Cp3	0.007467
	C_{34}	-0.009460	Cp4	-0.003017
	C_{35}	-0.001202	Cp5	-0.002481
	C_{36}	0.015771		

FIGURE (17)

THE CONFIGURATION OF THE π-$C_5H_5CoI(PPh_3)CF_2CF_3$ MOLECULE

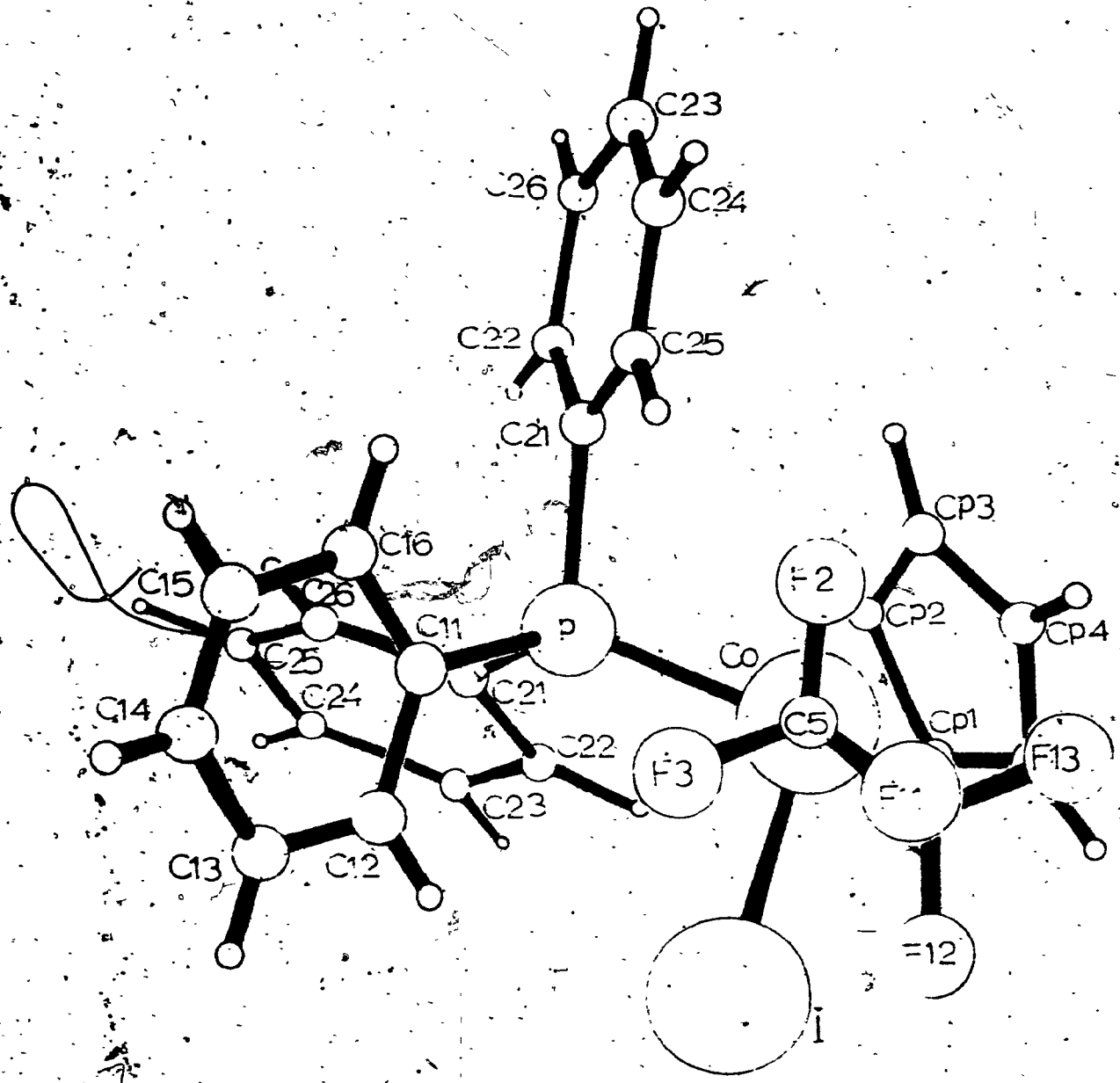
C23
C26
C24
C22
C25
C21
CP3
C16
C15
C26
F2
CP2
CP4
C11
P
Co
C25
C21
C24
C14
C5
Cp1
C22
F3
F13
C23
C13
C12
=12
I

FIGURE (18)

THE PACKING DIAGRAM OF π-$C_5H_5CoI(PPh_3)CF_2CF_3$

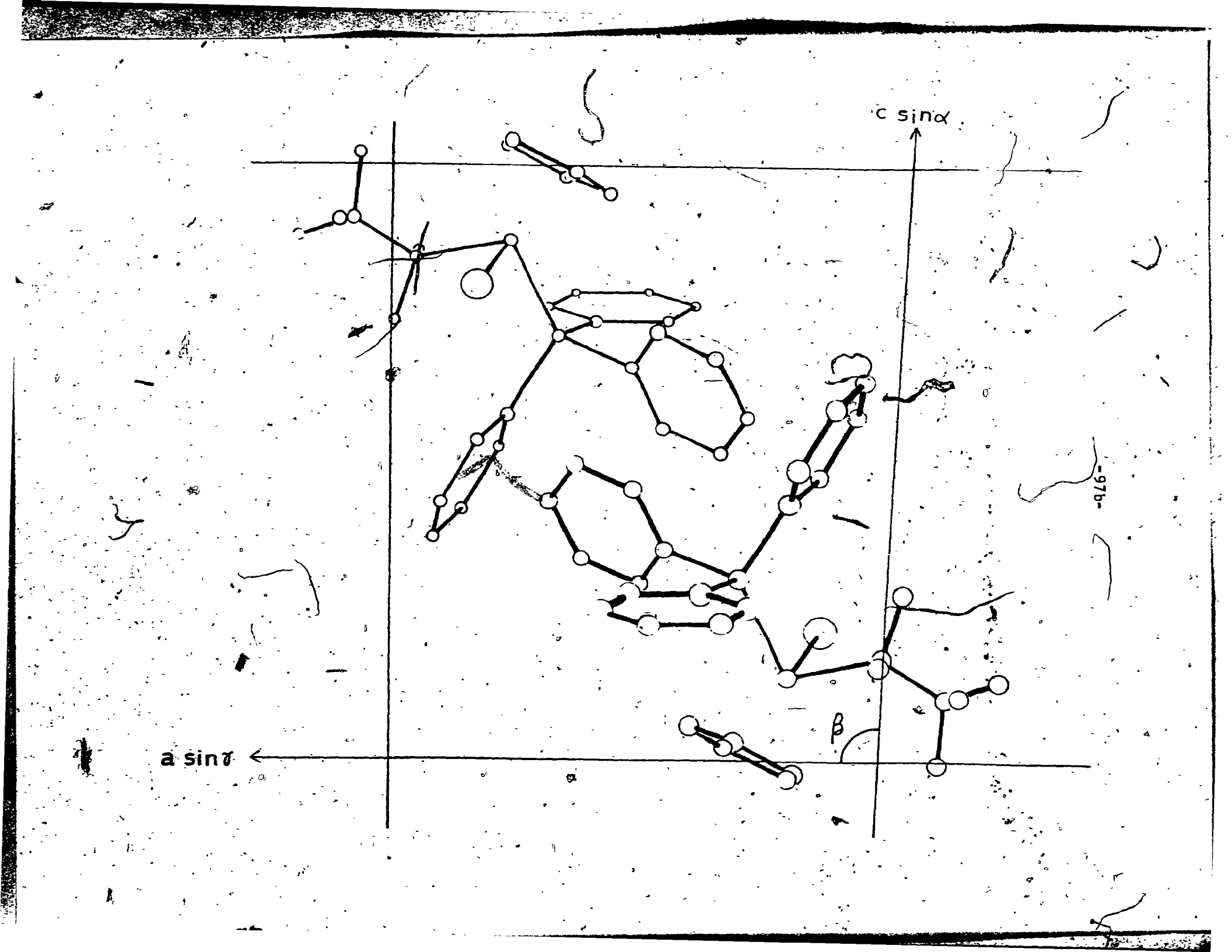
c sinα
a sinγ
β

SECTION IV DISCUSSION

(A) OVERALL GEOMETRY

Fluorfe 1, π-$C_5H_5Fe(CO)(PPh_3)CF(CF_3)_2$ and Fluorfe 2, π-$C_5H_5Fe(CO)(PPh_3)CF_2CF_3$ are similar compounds. In both compounds, the central iron atom is coordinated to a carbonyl group, a triphenyl phosphine molecule, and a cyclopentadienyl ring. A perfluoroisopropyl group is co-ordinated to the iron in Fluorfe 1 while a perfluoro-ethyl group is coordinated to the iron in Fluorfe 2.

Fluorco, π-$C_5H_5CoI(PPh_3)CF_2CF_3$ is a cobalt compound, the Co ion is coordinated to a iodine atom, a cyclopentadienyl ring, a triphenylphosphine, and a perfluoro-ethyl group.

The three compounds may be regarded as an pseudo octahedral complex of a metal ion (piano stool). The valence angles at the central metal atom of three compounds are as follows :

Fluorfe 1		Fluorfe 2		Fluorco	
C_4FeC_2	96°	C_1FeP	92°	$ICoC_5$	93°
$PFeC_2$	92°	$PFeC_2$	108°	$PCoC_5$	95°
C_4FeP	92°	C_1FeC_2	89°	ICoP	94°

These angles are close to 90°, just as in other semi-sandwich π complex for example, in the two 'isomers' of π-$C_5H_5FeI[P(OC_6H_5)_3]_2$ [7,8], the angles at the Fe atom have an average of 91.8°; in π-$C_5H_5Fe(CO)(PPh_3)(\sigma$-$C_6H_5)$ [1], angles

at the Fe atom have an average of 90.0°. In the molecule π-$C_5H_5Mn(CO)_3$(69), the valence angles $C_{carbonyl}$ — Mn — $C_{carbonyl}$ average 92±2°; whereas in the structure of π-$C_5H_5Rh(CO)(C_2F_5)I$, the corresponding anglesat the Rh atom (between the 'legs' of the stool), have an average of 89.1±1.0°.

(B) THE CYCLOPENTADIENYL RING

The cyclopentadienyl ring is planar in Fluorfe 1 and Fluorco (the maximum deviation of the carbon atoms from the plane of the ring is 0.007 Å in Fluorfe 1 and 0.009 Å in Fluorco).

The distance from the iron to the middle of the cyclopentadienyl ring is 1.7571 Å in Fluorfe 1 and Fe-C (cyclopentadienyl) distances are equal within the limits of the determination : the average distance is 2.14(1) Å which is longer than the distance found in sandwich complexes of the ferrocene type (2.06 Å)(67) and ferrocene derivatives. This increase relative to 'full' sandwich, however, is usual and is observed in nearly all half sandwich π complexes of the transition metals, attesting to the weakening of the π interaction between metal and cyclopentadiennyl ring. Thus in the structures $[\pi$-$C_5H_5Fe(CO)_2]_2$(14) and $[\pi$-$C_5H_5Fe(CO)_2]Sn(C_6H_5)_3$(15), the Fe — C (cyclopentadienyl) distances average 2.11Aand 2.095 Å. In $(\pi$-$C_5H_5)Fe(CO)[P(C_6H_5)_3](\sigma$-$C_6H_5)$, the average Fe — C(cyclopentadienyl) equals 2.10 Å.

The Fe — C(cyclopentadienyl) distances are apparently not equal in Fluorfe 2. They range from 1.85(5) to 2.08(5) Å. It is hard to say whether the ring is really tilted with respect to the iron atom, or whether this an artifact of the poor refinement.

In Fluorco, the C — C bonds in the cyclopentadienyl ring are equal within esds, range from 1.41 to 1.48 Å. The distance from the cobalt to the middle of the ring is 1.729 Å. The Co — C(cyclopentadienyl) distances are approximately equal, ranging from 2.09(1) to 2.14(1) Å, (average to 2.12(1) Å).

(C) THE CARBONYL MOIETIES

The M — C≡O moieties of Fluorfe 1 and 2 are not linear as frequently found.[18] The valence angle of Fe — C≡O is 170° in Fluorfe 1 and 176° in Fluorfe 2. A very general observation of the structures of metal carbonyls and metal-cyanides is that the M — C ≡ O and M — C ≡ N bond angles show systematic deviations from a value of 180° . A rationalization of this has been given for the case of $M(CO)_3$ fragments[70].

(D) THE TRIPHENYLPHOSPHINE GROUPS

The coordination of the P atom is distorted tetrahedral. In Fluorfe 1 and 2, the Fe — P bond lengths equal 2.25 Å and 2.20 Å respectively, which are close to those found in other iron phosphine complexes, e.g. $(\pi\text{-}C_5H_5)[P(C_6H_5)_3]Fe(CO)I$[1] (2.23 Å). Thus, in the present case, there is a considerable shortening of this bond in comparison with the sum (2.45 Å) of the covalent radii of iron (1.35 Å)[11] and phosphorus (1.10 Å)[12].

This shortening is an indication of the considerable dative interaction $d\pi(Fe) \rightarrow d\pi(P)$, which increases the multiplicity of the Fe — P bond (see introduction). This bond is even shorter (2.15 Å) in the two 'isomers'[7,8] of $(\pi\text{-}C_5H_5)Fe[P(OC_6H_5)_3]_2I$.

The chirality of the triphenylphosphine "propeller" in these compounds, is indicated on Figs 19a,b, and c. These figures are drawn with similar configuration at the metal assymetric centre. (It should be pointed out that the three crystal structures are all centrosymmetric, and contain both enantiomers). Fluorfe 2 and Fluorco are very similar compounds, differing only in the metal, and the substitution of I for CO in the latter. It is interesting to note therefore, that they represent "pseudo" diasteromers, and this observation lends some support to the explanation proposed for the C ≡ O stretching doublet in the I.R. of this type of compound.

(E) THE PERFLUOROALKYL GROUPS

The perfluoroisopropyl group in Fluorfe 1 and the perfluoroethyl group in Fluorco are in the staggered conformation as expected. The Fe — C_α distance in Fluorfe 1 is 2.06 Å; this shortening of metal- carbon(fluoroalkyl) bond length compared with metal-carbon(alkyl) is expected (see introduction) because of the $d\pi \rightarrow \sigma^*$ back donation. The averaged Fe — C_α — C_β angle in Fluorfe 1 is 113.1°. The increase in metal-carbon-carbon bond angle from the formal sp^3 angle of 109°28' is expected, this being a general phenomenon in transition metal fluoroalkyls as described before. Again, the Co — C_α — C_β, Co — C_α — F_2,

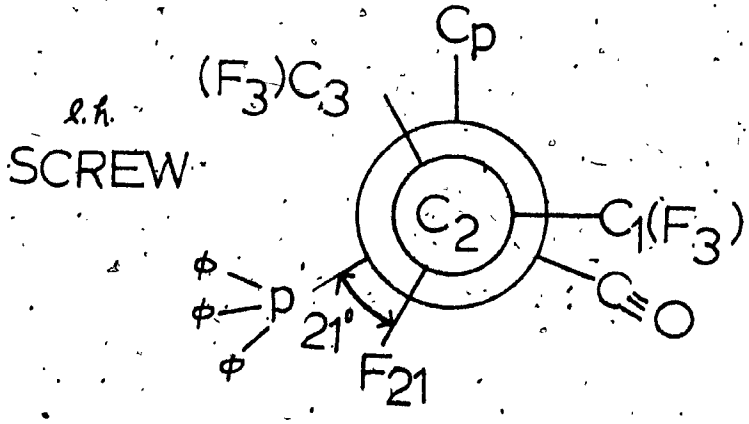

FIG.19 a

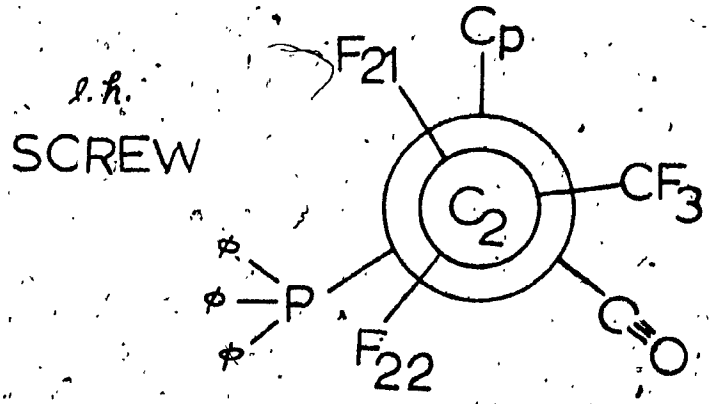

FIG.19 b

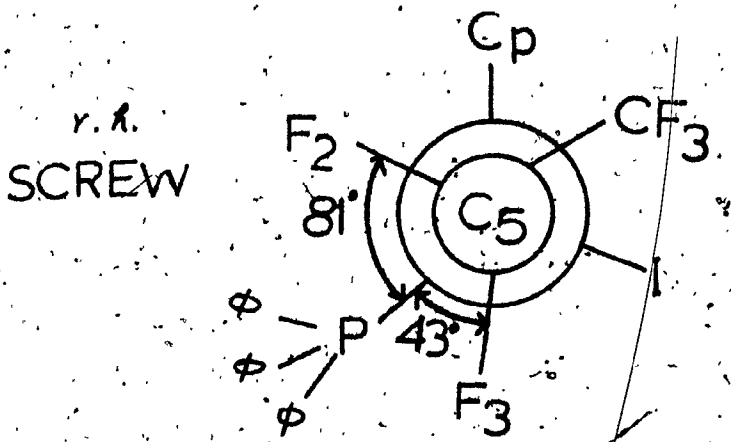

FIG.19 c

Co — C_α — F_3 angles in Fluorco are 120.2°, 109.6°, 112.7°, respectively, the increase of these angles from the regular tetrahedral value may be due to the increased repulsion of the electrons in the Co — C_1 bond from those in the C_1 — C_β, C_α — F_2, C_α — F_3 bonds. This evidence shows that π donation from metal dπ orbitals into C — F antibonding orbitals exists. Such shortening of Me — C_α bond and increase of the angles at C_α is also observed in π-$C_5H_5Rh(CO)(C_2F_5)I$.(6)

In Fluorfe 2, the perfluoroethyl group is also in a staggered conformation, the Fe — C_γ distance is equal to 2.07 Å, the Fe — C_α — C_β angle is 140°, but such a large deviation from the formal sp^3 angle of 109° is abnormal. The large increase of this angle cannot be caused by the electronic repulsions between the CF_2 and CF_3 group, and is presumably a further result of the poor refinement of this structure.

(F) MOLECULAR CONFORMATION

In Fluorfe 1, the angle between the planes defined by C_2 — Fe — P and F_{21} — C_2 — Fe is 21°, the slightly staggered conformation is shown in FIG(19a), see also FIG(13). The bulky triphenyl group is oriented in such a way that it is opposite to the two CF_3 groups and close to F_{21}. The conformation of Flurofe 2 is shown in FIG (19b), see also FIG(15); the CF_3 group lies remote from the Ph_3P group, closer to the CO group. Poor refinement precludes very exact conclusions regarding the dihedral angles.

In Fluorco, the angle between the planes defined by C_5 — Co — P and F_3 — C_5 — Co is 43°, the angle between the planes C_5 — Co — P and F_2 — C_5 — Co is 81°, the staggered conformation is shown in FIG(19c), see also FIG(17). In this triphenyl phosphine group is oriented opposite to the CF_3 and slightly closer to F_3, this can be rationalized by assuming that the CF_3 is closer to the less bulky atom I, as compared to the Cp ring.

These three conformations can be partly rationalized if it is assumed that the order of bulkiness is :

$$PPh_3 > Cp > I > CO.$$

SECTION V : CONCLUSION

Among the three crystal structures reported in this thesis, Fluorfe 1 and Fluorco can be considered satisfactory from the point of view of their accuracy. The third structure, Fluorfe 2, has not been well refined, and attempts to improve it have been defeated by difficutly in recrystallizing the small sample available (and the failure of the Baird group to repeat the preparation).

Further work might involve the estimation of the effect of intermolecular forces on the molecular conformations so that correlations between the observed crystal structure and the solution N.M.R. data could be justified or disallowed.

BIBLIOGRAPHY

(1) H.H. Jaffe and G.O. Doak, J. Chem. Phys., 21, 196 (1953).

(2) J. Chatt and B.L. Shaw, J. Chem. Soc. pp.705, 4020(1959); P.1718 (1960); P.285 (1961).

(3) J. Chatt, Record Chem. Progr. (Kresge-Hooker Sci. Lib.) 21, 147 (1960).

(4) P.M. Trichel and F,G.A. Stone, Advan. Organometal., 1, 178 (1964).

(5) M.R. Churchill, Inorg. Chem., 6, 185 (1967).

(6) M.R. Churchill, Inorg. Chem., 4, 1734 (1965).

(7) F.A. Cotton and J.A. McCleverty, J. Organometal. Chem. (Amsterdam), 4, 490 (1965).

(8) R. Mason and D.R. Russell, Chem. Commun. (London), 182(1965).

(9) M.J. Bennett and R. Mason, Proc. Chem.Soc., 273 (1963).

(10) J. Meunier-Piret, P. Piret, and M. Van Meerssche, Acta Cryst., 19, 85 (1965).

(11) N.W. Alcock, Chem. Commun. (London), 177 (1965).

(12) R.J. Gillespie and R.S. Nyholm, Quart. Rev. (London), 339 (1957).

(13) Cotton and Wilkinson, Advanced Inorganic Chemistry, Third Edition 740 (1972).

(14) G. Booth, Advances in Inorganic Chemistry and Radiochemistry, 6, 1 (1964).

(15) S.D. Robinson, Inorganic Chemistry, Series One, 6,121.

(16) H.J. Plastas, J.M. Stewart and S.O. Grim, J. Amer. Chem. Soc., 91, 4326 (1969).

(17) V.G. Andrianov and Yu.T. Struchkov, J. of Structural Chemistry, 9, pp.182,426, (1968).

(18) V.A. Semion and Yu.T. Struchkov, J. of Structural Chemistry, 10, 80 (1969).

(19) R.J. Doldens, W.T. Robinson, and J.A. Ibers, J. Amer. Chem. Soc., 89, 4323 (1967).

(20) L. Pauling, The Nature of the Chemical Bond, Cornell Univ. Press, Ithaca, New York, 3 rd. ed. (1960).

(21) F.A. Cotton and D.C. Richardson, Inorg. Chem., 5, 1851 (1966).

(22) J.H. Enemark and J.A. Ibers, Inorg. Chem., 6, 1575 (1967).

(23) J.A. Bertrand and D.L. Plymall, Inorg. Chem., 5, 879 (1966).

(24) J.M. Coleman and L.F. Dahl, J. Amer. Chem. Soc,, 89, 542 (1967).

(25) D.S. Brown and G.W. Bushnell, Acta Crystallogr., 22, 296 (1967).

(26) N.C. Stephenson, Acta Crystallogr., 17, 1517 (1964).

(27) N.C. Stephenson, J. Inorg. and Nucl. Chem., 24, Dec. 797 (1962).

(28) Donald E. Sands, "Introduction to Crystallography".

(29) G.H. Stout and L.H. Jensen, "X-Ray Structure Determination", Macmillan, New York, 1968.

(30) P.P. Ewald, "Fifty Years of X-Ray Diffraction", P.P. Ewal,ed., "International Union of Crystallography", Utrecht, The Netherlands, 1962, pp. 6-75.

(31) M.J. Buerger, "X-Ray Crystallography", Wiley, New York,1942.

(32) "The Precession Method in X-Ray Crystallography", Wiley, New York, 1964.

(33) "International Table for X-Ray Crystallography", Ed. K. Lonsdale, Kynoch Press, Birmingham, England, 1962. Vol.I.

(34) "The Optical Principles of the Diffraction of X-Rays", Cornell University Press, Ithaca, N.Y., 1965, pp.34-52.

(35) M.J. Buerger, "Crystal Structure Analysis", Wiley, New York, 1960 pp.29-48.

(36) (a) U.W. Arndt, Acta Cryst.,17, 1183 (1964); (b) S.C. Abrahams, Acta Cryst., 17, 1190 (1964); (c) L.E. Alexander and G.S. Smith, Acta Cryst.,17, 1195 (1964); (d) J. Ladell, Norelco Reptr., 12, 48 (1965); (e) U.W. Arndt and D.C. Philips, Acta Cryst., 14, 807 (1961); (f) L.E. Alexander and G.S. Smith, Acta Cryst.,15, 983 (1962); (g) U.W. Arndt and B.T.M. Williams, Single Crystal Diffractometry, Cambridge University Press, Cambridge, 1966.

(37) " The Optical Principles of the Diffraction of X-Rays", Cornell University Press, Ithaca, N.Y., 1965,pp.44-66.

(38) M.J. Buerger, "Crystal Structure Analysis", Wiley, New York, 1960, pp. 192-194.

(39) " International Table for X-Ray Crystallography", Ed. K. Lonsdale, Kynoch Press, Birmingham, England, 1962 Vol.III, pp. 137-139.

(40) M.J. Buerger, "Crystal Structure Analysis", Wiley, New York, 1960 pp.204-231.

(41) J.W. Jeffery and K.M. Rose, Acta Cryst., 17,343 (1964).

(42) W.R. Busing and H.A. Levy, Acta Cryst., 10, 180 (1957; J.de Meulenaer and H. Tompa, Acta Cryst., 19, 1014 (1965); P. Coppens, J.de Meulenaer and H. Tompa, Acta Cryst., 22, 601 (1967); and references therein.

(43) " The Optical Principles of the Diffraction of X-Rays", Cornell University Press, Ithaca, N.Y., 1965, pp.34-52.

(44) M.J. Buerger, "Crystal Structure Analysis", Wiley, New York, 1960 pp.231-237; "The Optical Principles of the Diffraction of X-Rays", Cornell University Press, Ithaca, N.Y., 1965, pp.193-267.

(45) A.J.C. Wilson, Nature, 150, 151 (1942).

(46) A.L. Patterson, Z. Krist., A 90, 517 (1935).

(47) H. Lipson and W. Cochran, "The Determination of Crystal Structures", G. Bell, London, 1957, pp. 12-15, 150-198.

(48) M.J. Buerger, "Vector Space", Wiley, New York, 1959 pp. 5-29, 41-64.

(49) E.T. Whittaker and G. Robinson, The Calculus of Observation, 4th ed., Blackie and Son, Glasgow, 1944, pp. 209-259; E.W. Hughes, J. Am. Chem. Soc., 63, 1737, (1941); W.C. Hamilton, Statistics in Physical Science, Ronald Press, New York, 1964, pp. 124-157; W.E. Deming, Statistical Adjustment of Data, Wiley, New York, 1943, pp. 14-58.

(50) H. Lipson and W. Cochran, "The Determination of Crystal Structures", G. Bell, London, 1957, pp. 76-109.

(51) M.J. Buerger, " Crystal Structure Analysis" Wiley, New York, 1960, pp. 370-508.

(52) J.S. Rollett, ed., "Computing Methods in Crystallography", Pergamon Press, Oxford, 1965, pp. 38-46.

(53) J.M. Robertson, "Organic Crystals and Molecules", Cornell University Press, Ithaca, N.Y., 1953, pp. 101-108.

(54) A.I. Kitaigorodskii, "The Theory of Crystal Structure Analysis", Consultants Bureau, New York, 1961.

(55) M.M. Woolfson, "Direct Methods in Crystallography", Oxford University Press, New York, 1961.

(56) J. Karle, " Advances in Structure Research by Diffraction Methods ", R. Brill and B. Mason, eds., Wiley-Interscience, New York, 1964, pp. 55-89.

(57) J. Karle and H. Hauptmann, Acta Cryst., 9, 635 (1956).

(58) D. Sayre, Acta Cryst., 5, 60 (1952).

(59) H. Lipson and W. Cochran, "The Determination of Crystal Structure", G. Bell, London, 1957, pp. 38-46.

(60) M.J. Buerger, " Crystal Structure Analysis", Wiley, New York, 1960, pp. 259-282.

(61) J.S. Rollett, ed., "Computing Methods in Crystallography", Pergamon Press, Oxford, 1965, pp. 38-46.

(62) M.I. Bruce and F.G.A. Stone, "Preparative Inorg. Reactions", V.4., p.177.

(63) R.B. King and M.B. Bisnette, J. Organometal. Chem., 2, 15, (1964).

(64) P.M. Treichel and G. Werber, Inorg. Chem., 4, 1098 (1965).

(65) M.K. Churchill and Fennessey, Chem. Commun., 695, 1966.

(66) R. Prins, Mol. Phys., 19, 603 (1970); J. Chem. Phys., 50, 4804 (1969); Chem. Comm. 280, (1970); C.B. Harris, Inorg. Chem., 7, 1517 (1968); M.D. Fayer and C.B. Harris, Inorg. Chem., 8, 2792 (1969); Y.S. Sohn, D.N. Hendrickson and H.B. Gray, J. Amer. Chem. Soc., 93, 3603 (1971).

(67) Cotton and Wilkinson, "Advanced Inorganic Chemistry", 3rd Edition, (1972).

(68 a,b) "International Tables for X-Ray crystallography", Ed., K. Lonsdale, Kynoch Press, Birmingham, England, 1962. a: p.202, b: p. 210.

(69) A.F. Berndt and R.E. March, Acta Cryst., 16, 118 (1963).

(70) S.F.A. Kettle, Inorg. Chem., 4, 1661 (1965).